Local response theory of surface plasmons in the space-charge layer of GaAs (110)
by Bingruo Xu

A thesis submitted in partial fulfillment of the requirements for the degree of Master of Science in Physics
Montana State University

Abstract:
We study surface plasmons and phonons on n-type semiconductors, for non-unifonn free-carrier density profiles, through use of the dielectric theory of electron-energy-loss spectroscopy and nonlocal description of the response of the electrons.

First, self-consistent calculations of the spatial variation of the conduction-election density near the surface of n-type GaAs are presented. Second, the dielectric function and effective dielectric function are discussed, in which the Thomas-Fenni model and the Debye-Huckel model are introduced. Third, the energy loss spectra for bulk free-carrier densities of (I) n0=1.2*10^17 cm^-3 (2) n0= 1.3*10^18cm^-3 (3) n0=1.5*10^18 cm^-3 have been calculated. For each value of n0, we consider three values of the surface charge density, Qs=-0.08, 0.0, and 0.08 in thermal units, and plot the variation with wavevector of the maximum of the loss function. By varying these parameters we investigate a wide range of charge-density profiles and surface potentials; for example' our deplation layers have widths of 50A, 75A and 100A. The results obtained with the local response theory are compared with Mills' results which come from a nonlocal theory.

LOCAL RESPONSE THEORY OF SURFACE PLASMONS IN THE SPACE-CHARGE LAYER OF GaAs (110)

by

Bingruo Xu

A thesis submitted in partial fulfillment
of the requirements for the degree

of

Master of Science

in

Physics

MONTANA STATE UNIVERSITY
Bozeman,Montana

May,1989

APPROVAL

of a thesis submitted by

Bingruo Xu

This thesis has been read by each member of the thesis committee and has been found to be satisfactory regarding content, English usage, format, citations, bibliographic style, and consistency, and is ready for submission to the College of Graduate Studies.

May 19, 1989
Date

John Hermanson
Chairperson, Graduate Committee

Approved for the Major Department

5/19/89
Date

Head, Major Department

Approved for the College of Graduate Studies

June 9, 1989
Date

Henry J Parsons
Graduate Dean

STATEMENT OF PERMISSION TO USE

In presenting this thesis in partial fulfillment of the requirements for a master's degree at Montana State University, I agree that the Library shall make it available to borrowers under rules of the Library. Brief quotations from this thesis are allowable without special permission, provided that accurate acknowledgment of source is made.

Permission for extensive quotation from or reproduction of this thesis may be granted by my major professor, or in his absence, by the Dean of Libraries when, in the opinion of either, the proposed use of the material is for scholarly purposes. Any copying or use of the material in this thesis for financial gain shall not be allowed without my written permission.

Signature Bingmo Xu

Date May 19, 1989

ACKNOWLEDGMENTS

The author gladly takes this oppurtunity to acknowledge Professor John C. Hermanson who suggested and supported the research here. His advice and patience and skillfull direction have always been deeply appreciated.

The author also acknowledges the sustained support by family and the entire Physics Department at Montana State University.

TABLE OF CONTENTS

LIST OF FIGURES

ABSTRACT

We study surface plasmons and phonons on n-type semiconductors, for non-uniform free-carrier density profiles, through use of the dielectric theory of electron-energy-loss spectroscopy and nonlocal description of the response of the electrons.

First, self-consistent calculations of the spatial variation of the conduction-election density near the surface of n-type GaAs are presented. Second, the dielectric function and effective dielectric function are discussed, in which the Thomas-Fermi model and the Debye-Huckel model are introduced. Third, the energy loss spectra for bulk free-carrier densities of (1) $n_0=1.2*10^{17}cm^{-3}$ (2) $n_0=1.3*10^{18}cm^{-3}$ (3) $n_0=1.5*10^{18}cm^{-3}$ have been calculated. For each value of n_0, we consider three values of the surface charge density, Q_s=-0.08, 0.0, and 0.08 in thermal units, and plot the variation with wavevector of the maximum of the loss function. By varying these parameters we investigate a wide range of charge-density profiles and surface potentials; for example' our deplation layers have widths of 50A, 75A and 100A. The results obtained with the local response theory are compared with Mills' results which come from a nonlocal theory.

CHAPTER 1

INTRODUCTION

In the past century the studies of materials have been mainly focused on bulk properties. The understanding of surfaces and fundamental surface related processes has become feasible only in the last 20 years since modern technologies were developed.

During the past 20 years, electron-energy-loss spectroscopy (EELS) in the reflection geometry has emerged as a reliable technique for studying clean or contaminated surfaces. In this techniqe, monochromatized electrons backscattered from the surface of a target material are analyzed in energy to detect losses and gains characteristic of surface plasmons or vibrational excitations. First restricted to conducting targets, high resolution EELS experiments have recently been successfully performed with insulators and semiconductors,[1] so that this technique is now generally applicable as a powerful spectroscopic tool for the study of any material surface.

Near the surface of a doped semiconductor, the carrier density often differs dramatically from that in the bulk. Depletion layers may be encountered as thick as a few hundred angstroms, within which the free-carrier density drops dramatically below that in the bulk, or accumulation layers which contain an excess of carriers near the surface. In the first part of this thesis, self-consistent calculations of the

spatial variation of the conduction-electron density near the surface of n-type GaAs is presented, for the case where the surface is charge neutral, or bears net positive or negative charge. The model smears the charge density produced by ionized donors in the bulk into a jellium background, and introduces the effect of surface charge through a uniform electric field emanating from the surface. In this part, the Schrodinger equation subject to Poisson's equation and Fermi statistics is solved. The Hartree approximation is used to describe the electron-electron interaction.[2]

Recently, an adequate theoretical approach to EELS was developed within the so-called dielectric theory,[3,4] where the electrons are considered as classical particles, while the absorption and emission of phonons or plasmons are treated quantum mechanically. In the theoretical description, the dielectric constant $\varepsilon(\mathbf{k},\omega)$ depends on frequency and wave vector. With retardation ignored, the frequency ω_s of the surface plasmon is determined through the relation $\varepsilon(\omega_s)=-1$. If ω_p is the plasma frequency of the free carriers, and ε_∞ the high-frequency dielectric constant, then[5,10]

$$\varepsilon(\omega)=\varepsilon_\infty-\omega_p^2/(\omega^2+i\gamma\omega)$$

and

$$\omega_s=\omega_p/(\varepsilon_\infty+1)^{1/2}.$$

Actually, ε depends not only on the frequency ω, but position z, since $\omega_p=4\pi n(z)e^2/m^*$ where m^* is the free-carrier effective mass. Calculations of n(z), the conduction electron density, are described in the first part of this thesis. If the 2D wave vector $\mathbf{k}$ is not zero, but is very small, ε also depends on $\mathbf{k}$. If we use the Thomas-Fermi model,[6] then

$$\varepsilon(k,\omega,z)=\varepsilon_\infty-\omega_p^2/[(\omega^2-0.6V_F^2k^2)+i\omega\gamma]$$

where V_F is the Fermi velocity and γ is a damping factor.[6]
If we use the Debye-Huckel model,[7] then

$$\varepsilon(k,\omega,z)=\varepsilon_\infty-\omega_p^2/[(\omega^2-6k^2)+i\omega\gamma]$$

In fact, GaAs has an infrared active transverse optical phonon at long wavelengths. The background dielectric constant then is frequency dependent, and of the form[8]

$$\varepsilon(\omega)=\varepsilon_\infty+(\varepsilon_0-\varepsilon_\infty)\omega_{To}^2/(\omega_{TO}^2-\omega^2-i\omega\gamma),$$

where ω_{TO} is the frequency of the long-wavelength transverse optical phonon, and ε_0 the static dielectric constant.

The dielectric theory can also be applied to anisotropic crystals, provided $\varepsilon(\omega)$ in the loss function is replaced by an appropriate effective dielectric function $\xi(\mathbf{k},\omega)$. In Ref. 9, it is shown that the relevant effective dielectric function is equal to the surface value of the ratio of the displacement vector perpendicular to the surface, and the projection of the electric polarization field onto the direction of the surface wave vector k. The quantity is

$$\xi(k,\omega,z)=i\mathbf{D}(\mathbf{k},\omega,z)\cdot\mathbf{n}/[\mathbf{E}(\mathbf{k},\omega,z)\cdot\mathbf{k}/k],$$

with $\mathbf{D}(\mathbf{k},\omega,z)=\varepsilon(\omega,z)\mathbf{E}(\mathbf{k},\omega,z)$, where $\varepsilon(\omega,z)$, the long-wavelength dielectric constant

of the material, which may be a function of the coordinate z, is determined by n(z).

In the regime of small-angle deflections, where surface plasmon contributions dominate the loss spectrum for back scattering from the surface of a simple semiconductor, the incident electron interacts with the excitations in the material through the fluctuating electric fields in the vacuum outside the material.[11] An incoming electron has an accompanying electric field which polarizes the medium. The induced field of polarization interacts back on the electron and damps its motion; in other words, the energy lost by the probing electron is dissipated by the medium. In this thesis the loss function will be dealt with classically. The amplitude of the induced field involves the factor $1/(\xi_0+1)$ where $\xi_0=\xi(z=0)$ is the effective surface dielectric function. The probability for energy loss will be proportional to this factor. A zero in the denominator of the loss function gives a peak in the loss spectrum.[9]

The position of the peak in the loss function is also calculated as a function of k , for the different values of the surface charge, for T=300K, and a carrier concentration of (1) $n_0=10^{18}cm^{-3}$ (2) $n_0=3*10^{17}cm^{-3}$. Dispersion curves, showing our results for the peak position vs. the wavevector, are plotted and compared with Mills' results.[12] In this thesis a local dielectric response description is applied, while Mills' results come from a full nonlocal description.

In summary, surface plasmons on n-type semiconductors are studied, for non-uniform free-carrier density profiles, through the use of a formalism describing electron-energy-loss spectroscopy. In the calculation of the inelastic cross section, the loss function $Im[-1/(\xi(k,\omega)+1)]$ is required as input. To derive the effective dielectric function, the dielectric function $\varepsilon(k,\omega,z)$ needs to be calculated first. But $\varepsilon(k,\omega,z)$ is directly related to n(z). Thus we must first determine the free-carrier density profile.

The thesis is organized as follows. Chapter 2 presents self-consistent calculations of depletion-and accumulation-layer profiles for a range of carrier concentrations in n-type GaAs, at room temperature. Many figures are presented for several cases. In Chapter 3 and Chapter 4, we discuss the theory of the dielectric function and the effective surface dielectric function. In Chapter 5 we present the theory of the electron-energy-loss cross section and results for the dispersion relation, and Chapter 6 is devoted to a summary of our many results and principal conclusions.

CHAPTER 2

SELF-CONSISTENT CALCULATION OF DEPLETION-AND ACCUMULATION-LAYER PROFILES

A uniformly doped n-type GaAs slab with thickness near 1400 A is considered. The undoped crystal is to be regarded as a neutral medium whose electrical effect is simply to provide a background dielectric constant ε_∞. We consider an electric field E outside the material and normal to its surface, due to surface charges. The electric field just inside the material will be E/ε. When we consider boundary conditions on the potential, we will use the fact that the field outside the material is larger by a factor ε than that used in the boundary condition for the field inside.

The dynamic system we consider is the sea of conduction electrons which are free to move under the influence of various forces. There are two types of force[13] that act on a conduction electron. The first type is the electrostatic force arising from the charge density of other conduction electrons, the uniform background of ionized donors, and the externally imposed uniform field. The second type is the exchange and correlation force. Exchange and correlation forces arise among conduction electrons due to dynamic and statistical correlations of their motion. We do not consider these forces here, since they are weak in our case.[14]

The system of equations includes Schrodinger's equation for the state of the conduction electrons, a constitutive equation giving the charge density in terms of

wavefunctions for the occupied states, and Poisson's equation giving the potential in terms of the charge density.

The single-particle wave functions are solutions[2] of an effective Schrodinger equation

$$\left[-\frac{h^2}{2m^*}\nabla^2 + V(z) \right] \Psi_\alpha(r) = E_\alpha \Psi_\alpha(r) \qquad (2.1)$$

where m^* is the effective mass; for GaAs, $m^*=0.069m$, with m the free-electron mass. V(z) is the self-consistent potential. The solution of this equation is of the form

$$\Psi_{k,i}(r) = [\exp(ik \cdot r)/A^{1/2}]\chi_i(z) \qquad (2.2)$$

where **k** is the wave vector parallel to the surface, A is the area of the sample and the index α represents the combination (k ,i), where i labels a particular solution for wave vector **k** . In Eq. (2.1),the energy zero is the conduction band edge.

$$E_\alpha = E_{k,i} = (h^2k^2/2m^*) + \varepsilon_i$$

The value of ε_i is discrete and can be positive or negative; we have then

$$\left[-\frac{h^2}{2m^*}\frac{d^2}{dz^2} + V(z) \right]\xi(z) = \varepsilon_i\chi_i(z) \qquad (2.3)$$

The solutions of Eq.(2.3) are subject to the boundary conditions

$$\chi_i(0) = 0 \tag{2.4a}$$

$$\chi_i(L) = 0 \tag{2.4b}$$

where L is the thickness of the slab.

The calculation is carried out in the Hartree approximation. It is assumed that the potential energy V(z) appearing in Schrodinger's equation is just the energy of an electron in the electrostatic potential $\Phi(z)$ set up by all the conduction electrons. The electrostatic potential satisfies Poisson's equation:

$$V(z) = - e\Phi(z) \tag{2.5}$$

$$-\frac{d^2\Phi(z)}{dz^2} = \frac{4\pi}{\varepsilon_s}\,\delta n(z), \tag{2.6}$$

where ε_s is the static dielectric constant, and $\delta n(z)$ is the deviation of the electron density from its bulk value. We chose the zero of energy such that $\Phi(L/2)=0$.

The boundary condition on the potential is

$$-\left(\frac{d\Phi}{dz}\right)_{z=0} = E_0 \tag{2.7}$$

There are two contributions to $\delta n(z)$,[2] so $\delta n(z)=\delta n_c(z)+\delta n_d(z)$. The first is from the free carriers in the conduction band:

$$\delta n_c(z) = \frac{2}{(2\pi)^2} \int d^2k \sum_i f\left[\frac{h^2k^2}{2m^*} + \varepsilon_i - \mu \right] \chi_i^2(z) - n_0 \qquad (2.8)$$

where $f\left[\frac{h^2k^2}{2m^*} + \varepsilon_k - \mu \right] = \left[\exp\left(\beta\left(\frac{h^2k^2}{2m^*} + \varepsilon_k - \mu \right)\right) + 1 \right]^{-1}$

is the Fermi-Dirac function with $\beta=(k_BT)^{-1}$, n_0 is the bulk free-carrier concentration and μ is the chemical potential.

The second contribution is

$$\delta n_D(z) = n_D \left[f\left(E_D - e\Phi(z) - \mu \right) - f\left(E_D - \mu \right) \right]$$

where n_D is the concentration of donor impurities. Except at the highest concentrations, we can assume that $\delta n_D(z)=0$, a constant. The self-consistent solution of Eqs. (2.3) and (2.6) proceeds as follows.

First, an initial potential is employed in the Schrodinger equation, which may then be solved straightforwardly by a series approach. Then $\delta n(y)$ may be constructed from these solutions. Finally, the potential $\Phi(z)$ is calculated. We repeat the procedure again and again until the new potential and old potential agree within the desired precision.

Before proceeding further, it is convenient to introduce the dimensionless units which will be employed for most of what follows. All energies will be expressed as multiples of k_BT and all lengths will be expressed as multiples of the thermal wave length

$$\lambda = (h^2/2m^*k_BT)^{1/2}$$

which assumes the value 46.2A for GaAs at room temperature. That is, we have

$$- e\Phi(y) = \Phi(y)k_BT \tag{2.8a}$$

$$z = y\lambda \tag{2.8b}$$

$$k \rightarrow k\,\lambda^{-1} \tag{2.8c}$$

$$\chi_i \rightarrow \chi_i\lambda^{-1/2} \tag{2.8d}$$

Schrodinger's equation (2.3) now takes the form

$$\left(- \frac{d^2}{dy^2} + \Phi(y) \right) \chi_i(y) = \varepsilon_i\chi_i(y) \tag{2.9}$$

Poisson's equation (2.6) becomes

$$- \frac{d^2\Phi}{dy_2} = - 8\pi \frac{\lambda}{a_0} \delta n(y) \tag{2.10}$$

where $a_0 = \varepsilon_s h^2/m^*e^2$ is the Bohr radius.

The boundary conditions and constraint on the charge density become

$$\Phi(y=L/2) = 0 \tag{2.11}$$

$$\left(\frac{d\Phi}{dy}\right)_{y=0+} = -8\pi\frac{\lambda}{a_0}Q \tag{2.12}$$

where $Q = -1/2\int_0^L \delta n(y)\, dy$ (2.13)

is the charge displaced by virtue of the presence of a depletion layer, or an accumulation layer. If we assume Q_s is the charge per unit area trapped on the surface, then Q_s must equal -Q to satisfy electrical neutrality. We can also obtain the electrostatic potential by integrating Eq. (2.10), noting the boundary conditions

$$\left[\frac{d\Phi(y)}{dy}\right]_{y=y} - \left[\frac{d\Phi(y)}{dy}\right]_{y=0+} = A\int_0^y \delta n(y')dy' \tag{2.14}$$

where $A=-8\pi\lambda/a_0$ and according to (2.12),

$$\Phi'(y)\big|_{y=0+} = -8\pi Q\lambda/a_0 = AQ = -A\int_0^\infty \delta n(y)dy \tag{2.15}$$

$$\Phi'(y) = A\int_0^y \delta n(y')dy' + \Phi'\big|_{y=0^+}$$

$$= A\int_0^y \delta n(y')dy' - A\int_0^\infty \delta n(y')dy'$$

$$= -A\int_y^\infty \delta(y')\, dy'$$

On the other hand, we also have

$$\Phi\big|_y^{\infty} = \int_y^{\infty} d\Phi(y') = \int_y^{\infty} \Phi'(y')\, dy'$$

$$= - A\int_y^{\infty} dy' \int_{y'}^{\infty} \delta n(y'')\, dy''$$

since $\Phi(\infty) = 0$, and thus

$$\Phi(y) = A\int_y^{\infty} dy' \int_{y'}^{\infty} \delta n(y'')\, dy''$$

$$= A\int_y^{\infty} dy'' \, \delta n(y'') \int_y^{y''} dy'$$

$$= A\int_y^{\infty} dy'' \, \delta n(y'') \, (y''-y)$$

Now let $x = y'-y$, $dy'' = dx$; then

$$\Phi(y) = A\int_0^{\infty} dx \, \delta n(x+y) \, x$$

$$= - 8\pi\lambda/a_0 \int_0^{\infty} dy' \, y' \, \delta(y+y') \qquad (2.16)$$

Finally we let $x = y'$. Eq.(2.16) is equivalent to Eq.(2.6).

The charge density or, more correctly, the number density appropriate to this unit of length is expressed by

$$\delta n(y) = 2\int_{-\infty}^{\infty} \frac{d^2k}{4\pi^2} \sum_i \frac{1}{\exp(\varepsilon_i+k-\mu)+1} \chi_i^2(y) - n_0 \qquad (2.17)$$

Since the electrostatic potential is symmetric,

$$\delta n(y) = \frac{1}{2\pi^2} \sum_i \int_{-\infty}^{\infty} \frac{d^2k}{\exp(\varepsilon_i + k^2 - \mu) + 1} \chi_i^2(y) - n_0$$

$$= \frac{1}{2\pi} \sum_i \ln \left[(\exp(\mu - \varepsilon_i) + 1 \right] \chi_i^2(y) - n_0 \qquad (2.18)$$

The Fermi level is found by requiring charge neutrality:

$$\int_0^L \delta n(y)\, dy = -2Q \qquad (2.19)$$

or

$$\frac{1}{2\pi} \sum_i \log \left[\exp(\mu - \varepsilon_i) + 1 \right] = n_0 L - 2Q \qquad (2.20)$$

In the numerical calculation, first a step charge density is used, with the thickness D of the depletion or accumulation layer determined by Q_s from the definition $n_0 D = Q_s$. Then this charge density is put into the equation

$$\Phi_i(y) = -8\pi\lambda/a_0 \int_0^{L/2-y} dy' y' \delta(y+y'),$$

where i means initial. After integration, the initial potential can be obtained. This potential is put into the Schrodinger equation (2.9); then, the wave function and the eigenvalues which can be positive or negative and also discrete are calculated. According to Eq. (2.18), the deviation of the electron density from its bulk value will be obtained.

In the next step, using the equation

$$\Phi_n(y) = - 8\pi\lambda/a_0 \int_0^{L/2-y} dy'y'\delta(y+y'),$$

where n means "new", again and integrating it, we obtain a new potential. Comparing the new potential with the initial potential, if the value $[\Phi_n(y)-\Phi_i(y)]$ is larger than the precision which we desire, we use some linear combination of these two potentials as input into the Schrodinger equation and repeat the procedure again and again until the value $[\Phi_n(y)-\Phi_i(y)]$ is equal or smaller than the precision which we desire. This concludes the self-consistent calculation.

Several bulk charge densities, namely $1*10^{17}/cm^3$, $3*10^{17}/cm^3$, $1.2*10^{18}/cm^3$ and $1.5*10^{18}/cm^3$ have been used in our calculations. For each charge density, different thicknesses of depletion and accumulation layers, namely 50A, 75A and 100A were used. Also, the potentials for different cases were calculated. These potentials describe the band bending in the surface region.

CHAPTER 3

BULK DIELECTRIC FUNCTION

Classical Plasma Frequency[33]

We now discuss collective electron motions based on a purely classical and elementary treatment of plasma oscillations. Let the uniform background density of positive charge be en_0, and let $n(\mathbf{r},t)$ be the density of electrons at position $\mathbf{r}$ at time t.

The excess positive charge is given by (n_0-n) and hence from Maxwell's equations

$$\nabla\cdot\mathbf{E} = 4\pi e\,(n_0 - n) \tag{3.1.1}$$

where E is the electric field.

Now, suppose the electron gas is displaced by x to give a current density nv; then according to the equation of continuity

$$\nabla\cdot(nv) = -\,\partial n/\partial t \tag{3.1.2}$$

It is assumed that the displacement x is small. Then the plasma oscillations are small in amplitude and Eq. (3.1.2) may be written as

$$n_0 \nabla \cdot v = - \partial n/\partial t \qquad (3.1.3)$$

which can be integrated to give

$$n_0 - n = n_0 \nabla \cdot x \qquad (3.1.4)$$

since $n=n_0$, at $x=0$. Thus, we have the result, from Eq.(3.1.1),

$$\nabla \cdot E = 4\pi e n_0 \nabla \cdot x \qquad (3.1.5)$$

and hence

$$E = 4\pi e n_0 x \qquad (3.1.6)$$

which satisfies the boundary condition that $E=0$ when $x=0$. Combining this with the Newtonian equation of motion for an electron in an electric field E,namely

$$m\ddot{x} = - eE \qquad (3.1.7)$$

we have

$$m\ddot{x} + 4\pi e^2 n_0 x = 0 \qquad (3.1.8)$$

This immediately shows that oscillations in the electron gas can occur, with angular frequency ω_p given by

$$\omega_p = (4\pi n_0 e^2/m)^{1/2} \qquad (3.1.9)$$

ω_p is called the plasma frequency

Frequency dependent dielectric constant $\varepsilon(\omega)$

Consider the jellium model, and apply a time-varying external field E. Under these circumstances, the equation of motion for an electron is, classically,

$$m\frac{d^2x}{dt^2} + m\gamma\frac{dx}{dt} = -eE \qquad (3.2.1)$$

where m is the electronic mass and e is the magnitude of the electronic charge. E is the electric field acting on the electron as a driving force. The term $m\gamma(dx/dt)$ represents viscous damping and provides for an energy loss mechanism. The electric field E can be taken to vary in time as $e^{-i\omega t}$, thus the solution to Eq. (3.2.1) is

$$x = \frac{eE/m}{\omega^2 + i\gamma\omega} \qquad (3.2.2)$$

and the induced dipole moment is

$$P = -ex = -\frac{e^2E}{m(\omega^2 + i\gamma\omega)} \qquad (3.2.3)$$

Note that it is important to be consistent in the form of the time variation used to describe time-dependent fields. The use of a time variation $e^{i\omega t}$ leads to a complex

refractive index n=n-ik, as we now show.

If there are n atoms per unit volume, the polarization is

$$\mathbf{P} = - \mathbf{np} = \frac{ne^2}{m(-\omega^2-i\gamma\omega)} \mathbf{E} = \chi E \qquad (3.2.4)$$

The complex dielectric function ε is defined by

$$n^2 = \varepsilon = \varepsilon_\infty + 4\pi\chi \qquad (3.2.5)$$

Using Eq. (3.2.4), this yields

$$\varepsilon(\omega) = \varepsilon_\infty - \frac{4\pi ne^2}{m(\omega^2+i\gamma\omega)} \qquad (3.2.6)$$

$$=\varepsilon_\infty - \omega_p^2/(\omega^2+i\gamma\omega)$$

From Eq.(3.2.6)[16]

$$\varepsilon_1(\omega) = n^2 - k^2 = \varepsilon_\infty - \frac{\omega_p^2(\omega^2)}{(\omega^2)^2+\gamma^2\omega^2} \qquad (3.2.7)$$

$$\varepsilon_2(\omega) = 2nk = \frac{\omega_p^2\gamma\omega}{(\omega^2)^2+\gamma^2\omega^2} \qquad (3.2.8)$$

Lindhard screening

Lindhard screening

Here, Lindhard screening[17] is discussed briefly. The plasma oscillations can exist because for small k, the dielectric function does not always act as a screening factor. The long-range Coulomb interactions then make possible collective oscillations of large numbers of electrons. The dielectric constant in the limit of long wavelengths has the Drude form

$$\varepsilon(\omega) = \varepsilon_\infty - \frac{\omega_p^2}{\omega^2 + i\gamma\omega}$$

But this is for the case k=0. If the phenomenon of screening is considered, the general dielectric constant is

$$\varepsilon(k) = 1 - \frac{4\pi}{k^2}\frac{\rho^{ind}(k)}{\Phi(k)} \qquad (3.3.1)$$

where ρ^{ind} is the charge density induced in the eletron gas by the external particle and $\Phi(k)$ is the total potential. If Φ varies slowly, we can use the Thomas-Fermi approximation; then the dielectric constant becomes

$$\varepsilon(k) = 1 + k_0^2/k^2 \qquad (3.3.2)$$

where $k_0^2 = 4\pi e^2(\partial n_0/\partial\mu)$ and n_0 is the charge density of the uniform positive background which is given by

$$n_0(\mu) = \int \frac{dk}{4\pi^3} \frac{1}{\exp[\beta(hk^2/2m)-\mu]} \qquad (3.3.3)$$

where μ is the chemical potential.

Another theory is due to Lindhard. In this case the induced density is required only to be of linear order in the total potential Φ. The dielectric constant is

$$\varepsilon(k) = 1 - \frac{4\pi e^2}{k^2} \int \frac{dq}{4\pi^3} \frac{f(\varepsilon_{q+k})-f(\varepsilon_q)}{(\varepsilon_{q+k}-\varepsilon_k)} \qquad (3.3.4)$$

where f denotes the equilibrium Fermi function for a free electron with energy $h^2k^2/2m$.

If the external field has time dependence $e^{-i\omega t}$, then the induced potential and charge density will also have such a time dependence, and the dielectric constant will depend on frequency as well as on wave vector. It can be generalized by using time-dependent rather than stationary perturbation theory. The Lindhard dielectric constant then becomes

$$\varepsilon(k,\omega) = \varepsilon_\infty + \frac{4\pi e^2}{k^2} \int \frac{dq}{4\pi^3} \frac{f(\varepsilon_{q+k}) - f(\varepsilon_q)}{(\varepsilon_{q+k} - \varepsilon_q) + h\omega} \qquad (3.3.5)$$

For the real part of this constant, following the procedure derived by Wooten,[18] the result is

$$\text{Re } \varepsilon(k,\omega) = \varepsilon_\infty - \frac{\omega_p^2}{} \frac{1}{} \qquad (3.3.6)$$

$$\omega^2 \quad 1\text{-}h^2k^2(3/5k_F^2)/m^2\omega^2$$

Using $hk_F/m = v_F$ where v_F is the velocity of an electron on the Fermi surface and assuming

$$h^2k^2(3/5k_F^2)/m^2\omega^2 << 1,$$

Eq.(3.3.6) becomes

$$\mathrm{Re}\varepsilon(k,\omega) \approx \varepsilon_\infty - \frac{\omega_p^2}{\omega^2}\left(1 + \frac{3k^2v_F^2}{5\omega^2}\right)$$

$$\approx \varepsilon_\infty - \frac{\omega_p^2}{(\omega^2 - 3k^2v_F^2/5)} \qquad (3.3.7)$$

In the numerical work, this formula will be used. It is called the Thomas-Fermi model.

Dielectric function including lattice vibrations

To describe the long wavelength optical vibrations, a coordinate specifying the relative displacement between the positive and negative ions is required. For an elastic motion, the effective inertial mass for a unit volume is the density; for the optical type of motion, on the other hand, the corresponding mass is the reduced mass of the positive and negative ions $M=(M_+*M_-)/(M_++M_-)$ divided by the volume of a lattice cell. It has been found that the most convenient parameter to choose for

describing the optical type of motion is the displacement of the positive relative to the negative ions multiplied by the square root of this effective mass per unit volume, which we denote by W:

$$\mathbf{W} = \rho^{1/2} (\mathbf{u}_+ - \mathbf{u}_-),$$

where $\rho = M/\Omega$, and Ω is the volume of a lattice cell.

For diatomic ionic crystals, the macroscopic theory is fully embodied in the following pair of equations:

$$d^2\mathbf{W}/dt^2 = - r_{11}\mathbf{W} + r_{12}\mathbf{E} \qquad (3.4.1)$$

$$\mathbf{P} = r_{12}\mathbf{W} + r_{22}\mathbf{E} \qquad (3.4.2)$$

where P and E are the dielectric polarization and electric field as defined in the usual way in Maxwell's theory.

The coefficients r_{11}, r_{12}, r_{22} are related to the dielectric function. The dielectric function for any particular frequency ω can be deduced directly from (3.4.1) and (3.4.2) by considering periodic solutions:

$$\mathbf{E} = \mathbf{E}_0 e^{-i\omega t} \qquad (3.4.3a)$$

$$\mathbf{P} = \mathbf{P}_0 e^{-i\omega t} \qquad (3.4.3b)$$

$$\mathbf{W} = \mathbf{W}_0 e^{-i\omega t} \qquad (3.4.3c)$$

Thus the results can be obtained from these equations

$$- \omega^2 W = - r_{11} W + r_{12} E \tag{3.4.4}$$

$$P = r_{12} W + r_{22} E \tag{3.4.5}$$

When W is eliminated from these equations, it is seen that P and E are related by

$$P = [r_{22} + r_{12}^2/(r_{11}-\omega^2)]E \tag{3.4.6}$$

Comparing it with the definition of the dielectric displacement,

$$D = E + 4\pi P = \varepsilon E,$$

the dielectric function is obtained:

$$\varepsilon(\omega) = 1 + 4\pi[r_{22} + r_{12}^2/(r_{11}-\omega^2)] \tag{3.4.7}$$

If $\omega^2 = \omega_0^2 = r_{11}$, there is a pole in this function, so r_{11} can be determined by this pole. ω_0 is in the infrared region. When $\omega << \omega_0$, $\varepsilon(\omega)$ reduces to the well-known static dielectric constant ε_0

$$\varepsilon_0 = 1 + 4\pi(r_{22} + r_{12}/r_{11}) \tag{3.4.8}$$

When $\omega >> \omega_0$, $\varepsilon = \varepsilon_\infty$, where ε_∞ is the high-frequency dielectric constant

$$\varepsilon_\infty = 1 + 4\pi r_{22} \tag{3.4.9}$$

Now, these cofficients can be found as

$$r_{11} = \omega_0^2 \tag{3.4.10a}$$

$$r_{12} = [(\varepsilon_0-\varepsilon_\infty)/4\pi]^{1/2}\omega_0 \tag{3.4.10b}$$

$$r_{22} = (\varepsilon_\infty-1)/4\pi \tag{3.4.10c}$$

Finally, the result is

$$\varepsilon(\omega) = \varepsilon_\infty + (\varepsilon_0-\varepsilon_\infty)\omega_0^2/(\omega_0^2-\omega^2) \tag{3.4.11}$$

If a simple damping term is considered, then Eq. (3.4.1) can be modified as

$$d^2W/dt^2 = - r_{11}W - \gamma W + \gamma_{12} \tag{3.4.12}$$

where γ is a positive constant with the dimension of frequency; the additional term repesents a force always opposed to the motion. So, Eq. (3.4.12) reduces to

$$-\omega^2 W = (-r_{11} + i\omega\gamma)W + \gamma_{12}E \tag{3.4.13}$$

The addition of the damping term is equivalent to the replacement of $-r_{11}$ by $r_{11}+i\omega\gamma$. Hence the dispersion formula (3.4.11) becomes[8,31]

$$\varepsilon(\omega) = \varepsilon_\infty + \frac{(\varepsilon_0-\varepsilon_\infty)\omega_0^2}{} \tag{3.4.14}$$

$$\omega_0^2 - \omega^2 - i\omega\gamma$$

Finally, the dielectric function including the Thomas-Fermi response is

$$\varepsilon(\mathbf{k},\omega) = \varepsilon_\infty - \frac{\omega_p^2}{(\omega^2 - 0.6V_F^2k^2) + i\omega\gamma} + \frac{(\varepsilon_0 - \varepsilon_\infty)\omega_0^2}{\omega_0^2 - \omega^2 - i\omega\gamma} \qquad (3.4.15)$$

CHAPTER 4

EFFECTIVE DIELECTRIC FUNCTION

The Maxwell equations for free modes are

$$\nabla \cdot \mathbf{D} = 0$$

$$\nabla \cdot \mathbf{B} = 0$$

$$\nabla \times \mathbf{E} = -\frac{1}{c}\frac{\partial \mathbf{B}}{\partial t}$$

$$\nabla \times \mathbf{H} = \frac{1}{c}\frac{\partial \mathbf{D}}{\partial t}$$

In EELS, retardation effects are negligible. So, we set $c=\infty$ in these equations. The electric field $\mathbf{E}(\mathbf{r},t)$ is Fourier transformed with respect to the coordinates x and y parallel to the surface and with respect to the time t:

$$\mathbf{E}(\mathbf{r},t) = \int d^2k \int_{-\infty}^{\infty} d\omega \; \mathbf{E}(\mathbf{k},\omega,z) \exp[i(k_x x + k_y - \omega t)] \qquad (4.1)$$

where $\mathbf{k}=(k_x,k_y)$ is a two-dimensional wave vector.

It is known that surface phonons in isotropic materials have frequencies ω such that $\varepsilon(\omega)=-1$, where $\varepsilon(\omega)$ denotes the bulk dielectric constant of the material. In the dielectric theory of EELS, these frequencies generate δ-like peaks in the so-called surface loss function $\mathrm{Im}[-1/(\varepsilon(\omega)+1)]$. It turns out that the dielectric theory can still be applied to anisotropic crystals, provided the loss function is replaced by an appropriate effective dielectric function $\xi(\mathbf{k},\omega,z)$, where $\mathbf{k}$ denotes the wave vector of the surface phonons. The effective dielectric function $\xi(\mathbf{k},\omega,z)$ is defined as[9,20]

$$\xi(\mathbf{k},\omega,z) = i\,\frac{\mathbf{D}(\mathbf{k},\omega,z)\cdot\mathbf{n}}{\mathbf{E}(\mathbf{k},\omega,z)\cdot\mathbf{k}/k} \tag{4.2}$$

where $\mathbf{D}(\mathbf{k},\omega,z)=\varepsilon(\omega,z)\mathbf{E}(\mathbf{k},\omega,z)$ and $\varepsilon(\omega,z)$, the dielectric constant of the material, is a function of the coordinate z. It is obvious that $\xi(\mathbf{k},\omega,z)$ will reduce to the bulk dielectric constant $\varepsilon(k,\omega)$ for an infinite isotropic medium.

Now the boundary condition at the surface is considered. The usual boundary conditions at interfaces are that the normal component of $\mathbf{D}$ and parallel component of E are continuous.

$$D_{\perp}(k,\omega,+0) = D_{\perp}(\mathbf{k},\omega,-0) \tag{4.3}$$

$$E_{\perp}(k,\omega,+0) = D_{\perp}(\mathbf{k},\omega,-0) - E_{e\perp}(\mathbf{k},\omega,0) \tag{4.4}$$

where $\mathbf{E}_e(\mathbf{r},t)=-\nabla V_e(\mathbf{r},t)$

From Eq. (4.2) we then have

$$E_{\perp}(k,\omega,+0) = -i\xi_0\mathbf{k}\cdot\mathbf{E}\,(\mathbf{k},\omega,-0)/k - E_{e\perp}(\mathbf{k},\omega,0)$$

$$= -i\xi_0 k[E(k,\omega,+0) + E_e(k,\omega,0)]/k - E_{e\perp}(k,\omega,0) \quad (4.5)$$

where $\xi_0 = \xi(k,\omega,-0)$. On the other hand, since for $z>0$ we have $\nabla\cdot E=0$, then

$$ik\cdot E(k,\omega,z)/k = E_\perp(k,\omega,z)$$

Using this relation, finally the result is[9]

$$(1+\xi_0)E_\perp(k,\omega,+0) = -i\xi_0 k\cdot E_e(k,\omega,0)/k - E_{e\perp}(k,\omega,0) \quad (4.6)$$

Since $V_e(k,\omega,z) = (8\pi)^{-1}\int dxdy \int_{-\infty}^{\infty} dt\ V_e(r,t)\exp[-i(k_x x+k_y y-\omega t)]$ and

$E_e = -\nabla V_e(r,t)$ we have

$$(1+\xi_0)E_\perp(k,\omega,+0) = -k\xi_0 V_e(k,\omega,0) + [\partial/\partial z\ V_e(k,\omega,z)]_{z=0} \quad (4.7)$$

If $V_e=0$, i.e. there is no external excitation, the electric field $E(k,\omega,z)$ equals zero in $z>0$ region, unless

$$\xi_0 = \xi(k,\omega,0) = -1 \quad (4.8)$$

This equation is a generalization of the well-known condition $\varepsilon(\omega)=-1$ giving the nonretarded eigen modes of a semi-infinite isotropic medium with dielectric constant $\varepsilon(\omega)$.[21]

Now a simple case is considered, in which ξ does not depend on the polar

angle of the two-dimensional wave vector k; this means the material is isotropic. In this case[9]

$$\xi(\mathbf{k},\omega,z) = [\frac{\varepsilon}{k}\frac{\partial}{\partial z} V(\mathbf{k},\omega,z)]/V(\mathbf{k},\omega,z) \qquad (4.9)$$

where $V(\mathbf{k},\omega,z) = (8\pi)^{-1} \int dxdy \int_{-\infty}^{\infty} dt\ V(\mathbf{r},t) \exp[-i(k_x x+k_y y-\omega t)]$. (4.10)

For free modes $\nabla\cdot\mathbf{D}=0$, so the Poisson equation is written as

$$\nabla\cdot(\varepsilon\mathbf{E}) = 0 \text{ i.e. } \nabla\cdot[\varepsilon(-\nabla V)] = 0,$$

so that

$$d/dz[\varepsilon(dV/dz)] - \varepsilon k^2 V = 0 \qquad (4.11)$$

Let us address the question how to solve the equation (4.9). Taking the derivative of both sides of Eq. (4.9) with respect to z,

$$\frac{d}{dz}\xi(z) = \frac{d}{dz}\{[\frac{\varepsilon(z)}{k}\frac{\partial}{\partial z} V(z)]/V(z)\},$$

the result is[9]

$$\frac{1}{k}\frac{d\xi(z)}{dz} + \frac{\xi^2(z)}{\xi(z)} = \varepsilon(z) \qquad (4.12)$$

This is called the Riccati equation for ξ. In the above procedure, we used the Poisson equation (4.11). For obvious typographical simplifications, we omit the $(\mathbf{k},\omega)$ dependence of ε and V and regard these quantities as functions of z.

In the numerical work, we imagine that the slab is cut into many layers. The thickness of each layer is the same. As a simplifying assumption, it is assumed that $\varepsilon(z)$ takes constant values in each layer. By this means an analytical expression for the effective dielectric constant $\xi_0(\mathbf{k},\omega)$ will be obtained.

We now attempt to solve the Riccati equation. The thicknesses of the layers i=1,2,3..., will be denoted by d_i which, together with the dielectric constants ε_i, specify the model.

By integrating the differential equation (4.12), the result is

$$-\frac{d\xi}{(\varepsilon^2-\xi^2)} = \frac{k}{\varepsilon}\,dz + c \text{ and}$$

$$\xi(z) = \varepsilon \tanh (kz + c)$$

where c is a constant. Then,

$$\xi(z) = \varepsilon \left[\frac{Ae^{kz}-A^{-1}e^{-kz}}{Ae^{kz}+A^{-1}e^{-kz}}\right] = \varepsilon \left[\frac{e^{kz}-A^{-2}e^{-kz}}{e^{kz}+A^{-2}e^{-1z}}\right]$$

where $A=e^c$. Now let $A^{-2} = (1-c')/(1+c')$, then

$$\xi(z) = \varepsilon \frac{C+\varepsilon\tanh(kz)}{} \qquad (4.13)$$

$$\varepsilon + C\tanh(kz)$$

where $C=c'\varepsilon$ is an arbitrary integration constant, and the solution of the Riccati equation in layer i can obviously be written as

$$\xi(z) = \varepsilon_i \frac{\xi_i+\varepsilon_i\tanh[k(z-z_i)]}{\varepsilon_i+\xi_i\tanh[k(z-z_i)]}, \quad z_i \le z \le z_{i-1} \tag{4.14}$$

In this equation, ξ_i denotes the value of $\xi(z_i)$ at the lower end z_i of the layer. By setting $z=z_{i-1}$ in Eq. (4.14), the following expression for ξ_{i-1} at the upper end z_{i-1} is obtained:

$$\xi_{i-1} = \xi(z_{i-1}) = \varepsilon_i \coth(kd_i) - \frac{[\varepsilon_i/\sinh(kd_i)]^2}{\varepsilon_i\coth(kd_i)+\xi} \tag{4.15}$$

This treatment is repeated in each layer, and since $\xi(z)$ is a continuous function of z, by construction, the continued-fraction expansion of ξ_0 is obtained, i.e., the effective dielectric function[9]

$$\xi_0 = a_1 - \cfrac{b_1^2}{a_1+a_2 - \cfrac{b_2^2}{a_2+a_3 - \cfrac{b_3^2}{a_3+a_4-\ldots}}} \tag{4.16}$$

where we have defined

$$a_i = \varepsilon_i\coth(kd_i) \tag{4.17}$$

$$b_i = \varepsilon_i/\sinh(kd_i) \tag{4.18}$$

When the ε_i assume positive imaginary parts, $1/(\xi+1)$ is a so-called positive-definite continued fraction. Obviously, if kd_i is infinite, then a_i will be ε_i and b_i will be zero. Eq. (4.16) is easy to deal with on a computer.

CHAPTER 5

ELECTRON-ENERGY-LOSS SPECTROSCOPY

Electron-energy-loss spectroscopy

In this section the theory of electron-energy loss in a reflection geometry for small-angle inelastic scattering from a medium is presented. In this theory, EELS can be treated within the framework of the so-called dielectric theory.[4] The electrons are considered as classical particles, while the absorption or emission of phonons or plasmons are quantum-mechanically described.[22,23] So, this theory is a semiquantum theory. The theory of the inelastic cross section was discussed some years ago[24,25] for scattering off the surface of a semi-infinite material. Unless the losses of interest lie in the range of several electron volts, very-high-resolution spectroscopic techniques are required.

The trajectory analysis proceeds by noting that an incoming electron polarizes the material, here viewed as a dielectric medium. The induced polarization produces an electric field which does work on the electron as it approaches. One calculates the total work performed by the induced field to obtain the total energy loss suffered by the electron, and an appropriate decomposition of this expression yields the energy distribution of those electrons which suffer an inelastic scattering.

The dielectric theory proceeds in two steps. The first step consists in evaluating

the work done by the polarization field of the sample on the electron. The work done is[9,12]

$$W = - e \int_{-\infty}^{\infty} \mathbf{V}_e(t) \cdot \mathbf{E}(\mathbf{r}_e(t),t)\, dt \qquad (5.1)$$

where $\mathbf{r}_e(t)$ is the trajectory of the electron (charge e). $\mathbf{V}_e(t)$ is the electron velocity, and $\mathbf{E}(\mathbf{r},t)$ denotes the polarization field of the material.

Let the electron trajectory be described by

$$\mathbf{r}_e(t) = t\mathbf{v}_p + |t\mathbf{v}_\perp|\mathbf{n} \qquad (5.2a)$$

with $\mathbf{v}_p$ the projection of $\mathbf{v}$ onto a plane parallel to the surface; $\mathbf{v}_\perp$ is the normal component of the velocity, and $\mathbf{n}$ denotes the unit outward normal at the surface. If the electron strikes the surface at t=0, then

$$z(t) = -v_\perp t \text{ for } t<0$$

$$z(t) = v_\perp t \text{ for } t>0 \qquad (5.2b)$$

We have chosen the convention that the coordinate z is parallel to the outward normal n, the surface coinciding with the plane z=0; negative z corresponds to the material region.

Eq. (5.2a) neglects the perturbation of the classical trajectory. That means the force of the polarization field does not affect the dynamics of the electron. Also, the penetration of the electron below the assumed abrupt surface is ignored.

Using Eq. (4.1), we have for the polarization field

$$E(\mathbf{r},t) = \int d^2k \int_{-\infty}^{\infty} d\omega E(\mathbf{k},\omega,z)\exp[i(k_x x+k_y y-\omega t)]$$

Before calculating the work, two useful equations are introduced. Here the retardation effects in the electric field are ignored. The first equation is

$$\nabla\times\mathbf{E}(\mathbf{r},t) = 0$$

Taking into account Eq. (4.1) and the identity

$$\nabla\times(\psi\mathbf{a}) = (\nabla\psi)\times\mathbf{a} + \psi\nabla\times\mathbf{a}$$

We have the result

$$\nabla\times\mathbf{E}(\mathbf{k},\omega,z) = -i\mathbf{k}\times\mathbf{E}(\mathbf{k},\omega,z) \qquad (5.3)$$

Eq.(5.3) is multiplied by $\mathbf{n}$ which is the unit vector in the z direction; taking into acount $\nabla\times\mathbf{E}=\partial/\partial z(-E_y\mathbf{i} + E_x\mathbf{j})$, we have the results

$$(\partial/\partial z)\mathbf{E} = i\mathbf{k}\,E_\perp \qquad (5.4a)$$

$$E_p = -iE_\perp \qquad (5.4b)$$

In the same way, from the condition $\nabla\cdot\mathbf{E}=0$ $(z>0)$, we obtain

$$(\partial/\partial z)E_\perp = -i\mathbf{k}\cdot\mathbf{E} \qquad (5.4c)$$

Taking into account Eq. (4.1), now, the expression for the classical work W is derived:

$$W = -e \int_{-\infty}^{\infty} \mathbf{V}_e(t)\cdot\mathbf{E}(\mathbf{r}_e,t)dt$$

$$= -e\int_{-\infty}^{\infty}dtV_e(t)\int d^2k\{\int_{-\infty}^{0}d\omega E(k,\omega,z)\exp[i(\mathbf{k}\cdot\mathbf{r} -\omega t)]$$

$$+\int_0^{\infty}d\omega E(k,\omega,z)\exp[i(\mathbf{k}\cdot\mathbf{r} -\omega t)]\}$$

$$= -e\int_{-\infty}^{\infty}dtV_e(t)\int d^2k 2\mathrm{Re}\int_0^{\infty}d\omega\ E(k,\omega,z)\exp[i(\mathbf{k}\cdot\mathbf{r} -\omega t) \qquad (5.5)$$

Here, the relation $E(-k,-\omega,z)=E^*(k,\omega,z)$ was used.

The expression for the energy lost by the electron may be cast into the form[9]

$$W = \int d\omega\ h\omega\ P(\omega) \qquad (5.6)$$

where $h\omega$ denotes the energy loss and $P(\omega)$ is interpreted as the probability per unit frequency that the electron has lost the energy $h\omega$. Comparing Eq. (5.5) with Eq. (5.6) and taking into account Eq. (5.2a),

$$P(\omega) = (2e/h\omega)\int_{-\infty}^{\infty}dtV_e(t)\cdot\int d^2k\ \mathrm{Re}\{E(k,\omega,z)\exp[i(\mathbf{k}\cdot\mathbf{r} -\omega t)]\}$$

$$= (-2e/h\omega)\mathrm{Re}\omega_{-\infty}^{\infty}dt\int d^2k\ [\mathbf{V}_p\cdot\mathbf{E}_p(k,\omega,z)+$$

$$V_\perp E_\perp(k,\omega,z)(|t|/t)]\exp[i(\mathbf{k}\cdot\mathbf{r} -\omega t)]$$

Taking into account Eq. (5.2a), Eq. (5.4a), then integrating by parts

$$\mathrm{Re}\int_{-\infty}^{\infty} \mathbf{v}_p \cdot \mathbf{E}_p(\mathbf{k},\omega,z)\exp[i(\mathbf{k}\cdot\mathbf{v}_p-\omega)t$$

$$=\mathrm{Re}\{-2i/(\mathbf{k}\cdot\mathbf{v}-\omega)\int_0^{\infty} \mathbf{v}\cdot\mathbf{k}\, E_\perp(\mathbf{k},\omega,z)\sin[(\mathbf{k}\cdot\mathbf{v}-\omega)z/v_\perp]dz\} \text{ and}$$

$$\mathrm{Re}\int_{-\infty}^{\infty} v_\perp(|t|/t)E_\perp(\mathbf{k},\omega,z(t))\exp[i(\mathbf{k}\cdot\mathbf{v}-\omega)t]dt$$

$$= 2\mathrm{Re}\int_0^{\infty} E_\perp(\mathbf{k},\omega,z(t))i\sin[(\mathbf{k}\cdot\mathbf{v}-\omega)z/v_\perp]dz,$$

we obtain the following result:

$$P(\omega) = \frac{-4e}{h\omega}\,\mathrm{Re}\int d^2k\int_0^{\infty}\left[\frac{-\mathbf{k}\cdot\mathbf{v}}{\mathbf{k}\cdot\mathbf{v}-\omega t} + 1\right]E_\perp(\mathbf{k},\omega,z(t))i\,\sin[(\mathbf{k}\cdot\mathbf{v}-\omega)z/v_\perp]dz$$

$$= \int \frac{4e}{h(\mathbf{k}\cdot\mathbf{v}-\omega)}\, d^2k\int_0^{\infty}\sin[(\mathbf{k}\cdot\mathbf{v}-\omega)z/v_\perp]\mathrm{Im}E_\perp(\mathbf{k},\omega,z(t))dz \qquad (5.7)$$

Integration by parts, complemented by the condition $\nabla\cdot\mathbf{E}(\mathbf{r},t)=0$ $(z>0)$ i.e. (5.4c) and $i\mathbf{k}\cdot\mathbf{E}=E_\perp k$, gives the result

$$P(\omega) = \int \frac{-4ev_\perp}{h(\mathbf{k}\cdot\mathbf{v}_p-\omega)^2} d^2k\{-\mathrm{Im}E_\perp(\mathbf{k},\omega,+0)+\frac{v_\perp}{(\mathbf{k}\cdot\mathbf{v}_p-\omega)}\int_0^{\infty}\sin[(\mathbf{k}\cdot\mathbf{v}_p-\omega)z/v_\perp]\cdot$$

$$\mathrm{Im}(-i\mathbf{k}\cdot i\mathbf{k}E_\perp)dz\} \qquad (5.8)$$

Comparing Eq. (5.8) with Eq. (5.7), we have[9]

$$P(\omega) = \mathrm{Im}\left[\frac{4ev_\perp}{h}\int \frac{E_\perp(k,\omega,+0)}{(\mathbf{k}\cdot\mathbf{v}_p-\omega)^2+(kv_\perp)^2}\,d^2k\right] \tag{5.9}$$

According to Eq. (4.7), it is obvious that before Eq. (5.9) can be evaluated, $V_e(\mathbf{k},\omega,0)$ and $\partial V_e/\partial z$ must be calculated. The Coulomb potential is

$$V_e(\mathbf{r},t) = -\,e/|\mathbf{r}-\mathbf{r}_e(t)| \tag{5.10}$$

It is obvious that we have

$$\nabla^2 V_e(\mathbf{r},t) = 4\pi e\delta(\mathbf{r}_p-\mathbf{r}_{ep}(t))\delta(z-z_e(t)) \tag{5.11}$$

where $\mathbf{r}_p$ and $\mathbf{r}_{ep}$ are the space vectors parallel to the surface. The coulomb potential is Fourier transformed with respect to $\mathbf{r}_p$:

$$V(\mathbf{r},t) = 1/2\pi \int_{-\infty}^{\infty} V_e(k,z,t)\, \exp[i(\mathbf{k}\cdot\mathbf{r}_p)]d^2k \tag{5.12}$$

Putting Eq. (5.12) into Eq. (5.11) and recalling the Fourier transform of the δ function, the result is

$$(d^2/dz^2 - k^2)V_e(k,z,t) = e/\pi\, \exp[-i\mathbf{k}\cdot\mathbf{r}_{ep}(t)]\delta(z-z_e(t)) \tag{5.13}$$

The solution of Eq. (5.13) is

$$V_e(\mathbf{k},z,t) = A\theta(z-z_e(t))\exp[-k(z-z_e(t))] - B\theta(z_e(t)-z)\exp[-k(z_e(t)-z)] \tag{5.14}$$

where A and B are the cofficients which can be determined by

$$dV_e/dz = A\delta(z-z_e(t)) + A\theta(z-z_e(t))(-k)\exp[-k(z-z_e(t)] + B\delta(z_e(t)-z) + B\theta(z_e(t)-z)(k)\exp[-k(z_e(t)-z)] \quad (5.15)$$

and

$$d^2V_e/dz^2 = A\delta'(z-z_e(t))-A\delta(z-z_e(t))k+Ak^2\theta(z-z_e(t))\exp[-k(z-z_e(t))] - B\delta'(z-z_e(t))-B\delta(z_e(t)-z)k+Bk^2\theta(z_e(t)-z)\exp[-k(z_e(t)-z)] \quad (5.16)$$

Putting Eq. (5.16) into Eq. (5.13) and comparing both sides, we have

$$A = B$$

and

$$A = [-\exp(-i\mathbf{k}\cdot\mathbf{r}_{ep}(t))]/2\pi k \quad (5.17)$$

Finally, we obtain the following result

$$V_e(\mathbf{k},z,t) = -e/2\pi k\{\theta(z-z_e(t))[\exp(-kz+kv_\perp|t|-i\mathbf{k}\cdot\mathbf{v}_p t] + \theta(z_e(t)-z)[\exp(kz-kv_\perp|t|-i\mathbf{k}\cdot\mathbf{v}_p t)]\} \quad (5.18)$$

where $z_e(t) = v_\perp |t|$. It is considerd that if

$$z - v_\perp |t| > 0 \qquad \text{for } t>0 \qquad t<z/v_\perp$$

$$\text{for } t<0 \qquad t>-z/v_\perp \tag{5.19a}$$

and if

$$z - v_\perp |t| < 0 \qquad \text{for } t>0 \qquad t>z/v_\perp$$

$$\text{for } t<0 \qquad t<-z/v_\perp \tag{5.19b}$$

The final results for V and dV/dz at z=0 are

$$V(k,\omega,0) = \frac{-ev_\perp}{2\pi^2[(kv_\perp)^2+(\omega-k\cdot v_p)^2]} \tag{5.20}$$

$$dV(k,\omega,0)/dz = \frac{-ekv_\perp}{2\pi^2[k^2v_\perp{}^2 + (\omega-k\cdot v_p)^2} \tag{5.21}$$

The final result for $E_\perp(k,\omega,0)$ is then

$$E_\perp(k,\omega,+0) = \frac{-1}{(1+\xi_0)} \cdot \frac{kv_\perp e}{\pi^2[(kv_\perp)^2+(\omega-k\cdot v_p)^2]} \tag{5.22}$$

The Eq. (5.9) now becomes

$$P(\omega) = \frac{4e^2 v_\perp^{\,2}}{\pi^2 h} \int \frac{k}{[(kv_\perp)^2+(\omega-k\cdot v_p)^2]^2} \, \mathrm{Im} \frac{-1}{\xi_0(k,\omega)+1} \, d^2k \qquad (5.23)$$

Upon noting that $\xi_0(k,\omega)$ depends only on the magnitude and not the direction of $\mathbf{k}$, Eq. (5.23) is[9]

$$P(\omega) = \frac{4e^2 v_\perp^{\,2}}{h\pi^2} \int dk\, k^2 \, \mathrm{Im} \frac{-1}{\xi_0(k,\omega)+1}$$

$$\cdot \int_0^{2\pi} d\theta \; 1/[(v_\perp k)^2+(\omega-kv_p\cos\theta)^2]^2 \qquad (5.24)$$

This integral on θ may be evaluated in closed form. Since this integral is encountered frequently in the theory of small-angle electron-energy loss, we shall quote the result explicitly. Let θ_I be the angle of incidence of the electron beam measured relative to the normal to the surface. Then

$$v_p = v_0 \sin\theta_I \qquad (5.25a)$$

and

$$v_\perp = v_0 \cos\theta_I \qquad (5.25b)$$

where v_0 is the speed of the incoming electron. Here, it is supposed that $\sin\theta_I = \cos\theta_I \equiv A$

In the numerical work, the result is conveniently expressed in term of the dimensionless variable x given by $x=kv_0/\omega$. The energy loss spectrum then becomes,

$$P(\omega) = \frac{4v_0^2e^2}{\pi h\omega^4A^2}\int \frac{dk\ k^2\ Im[-1/(\xi_0(k,\omega)+1)]}{x^3[(x^2-1)+4x^2A^2]^{1/2}} \qquad (5.26)$$

$$\cdot Re\{(x^2-1+2ixA)^{1/2}[(1+2x^2A+ixA)(1+x^2A^2)+x^2A^2(3x^2A^2-2-ixA)+x^4A^4]\}$$

We choose the incident-electron kinetic energy to be 9eV with 45^0 angle of incidence. The spectrometer slit widths are assumed equal to 1^0. The electron energy width γ is equal 10 meV and the phonon energy width Γ 0.3meV. We have calculated the energy loss spectrum Eq. (5.26) for charge densities of (1) $3*10^{17}cm^{-3}$ (2) $1*10^{18}cm^{-3}$ (3) $1.2*10^{18}cm^{-3}$ (4) $1.3*10^{18}cm^{-3}$ (5) $1.5*10^{18}cm^{-3}$. For those cases, depletion and accumulation layers were investigated using different thickness, namely 50A, 75A and 100A.

Dispersion of surface plasmons

In the above discussion, the material was assumed to be described by a dielectric constant which depends not only on the frequency ω, but position z, with the z axis normal to the surface. The dependence on z arises from the free carrier contribution $-4\pi n(z)e^2/m^*\omega^2$ with n(z) the local electron density at point z. Thus if $\mathbf{D}(\mathbf{r},\omega)$ and $\mathbf{E}(\mathbf{r},\omega)$ are the displacement and electric fields and $\varepsilon(z,\omega)$ the dielectric function, we have $\mathbf{D}(\mathbf{r},\omega)=\varepsilon(z,\omega)\mathbf{E}(\mathbf{r},\omega)$. One may question the quantitative validity of such a model, since the thickness of the depletion or accumulation layer is typically comparable to the Thomas-Fermi screening length. Under these conditions $\mathbf{D}(\mathbf{r},\omega)$ is

not proportional to $E(\mathbf{r},\omega)$ evaluated at the same point, but instead is an average over values of $E(\mathbf{r},\omega)$ throughout a volume whose linear dimension is the order of the screening length. A nonlocal description of the response of the electron gas should be employed.[12]

Ehlers and Mills studied surface plasmons on n-type semiconductors, for realistic and nonuniform free- carrier density profiles, and through use of a nonlocal description of the response of the conduction electrons. For three values of Q_s, i.e.,- 0.08, 0.0 and 0.08, they plotted the variation with k of the maximum of the loss function for different charge densities, namely $1*10^{17}cm^{-3}$, $3*10^{17}cm^{-3}$ and $1*10^{18}cm^{-3}$.

For these different charge densities and different Q_s, in this thesis, the Thomas-Fermi model and the Debye-Huckel model belonging to local response theory[26,27,28] are used to calculate the plasmon dispersion relation from the position of the peak in the loss function as a function of k.

The Thomas-Fermi model was introduced in Chapter 3. Now the Debye-Huckel model is introduced. This model is appropriate to study the collective oscillations of a system in thermodynamic equilibrium. The real part of the dielectric constant in the Debye-Huckel model is given by[29]

$$\mathrm{Re}\varepsilon(\mathbf{k},\omega) \approx 1 - \omega_p^2/\omega^2(1+3k^2k_BT/m\omega^2)$$

$$\approx 1 - \omega_p^2/(\omega^2-3k^2k_BT/m) \qquad (5.27)$$

The inelastic cross-sections have been calculated, so there is no difficulty to calculate the dispersion relations.

Many results, including depletion-and accumulation-layer profiles inelastic cross-sections and dispersion relations will be shown in Chapter 6.

CHAPTER 6

RESULTS AND CONCLUSION

In Fig. 1, the relation between the carrier concentration n_0 and the chemical potential is shown. Using Fig. 1, for a wide range of n_0, we can get the chemical potential directly.

Figures 2 and 3 show the charge density profiles and potential for $n_0=3*10^{17}cm^{-3}$; the results for $n_0=1*10^{18}cm^{-3}$ are given in Figs. 4 and 5. In Fig. 2 and Fig. 4, it is obvious that if Q is positive, there is a depletion layer, and the potential decreases monotonically to zero. When Q is decreased, the potential will become an attractive well at some point; this happens for positive Q, when V(0) is positive. The scheme breaks down just as the potential first crosses zero, to form the attractive well.

In Fig. 3 and Fig. 5, one notes that the flat band condition does not occur at Q=0, but there is a kind of dipole layer present near the surface, with a sign such that the surface potential is depressed below the bulk value. Since the wave functions of all electrons must drop to zero at the surface, there is a deficit of charge in a layer with thickness of roughly λ, and this must be compensated by a pileup of excess charges a bit farther into the crystal. It is evident that greatest sensitivity to the free carrier profile occurs when $k \cdot d \sim 1$, with d the thickness of the transition region between the surface and the bulk.

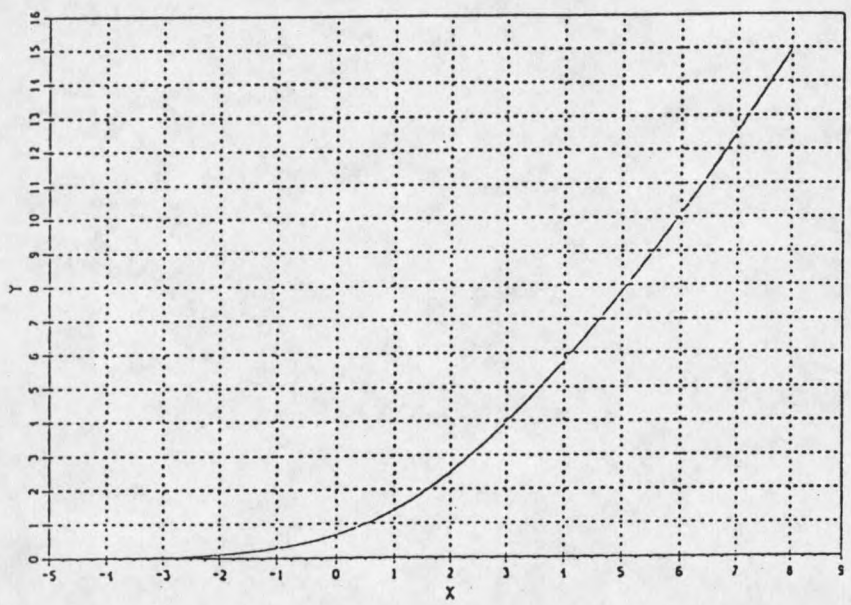

Fig. 1 Relation between the carrier concentration n and the chemical potential.

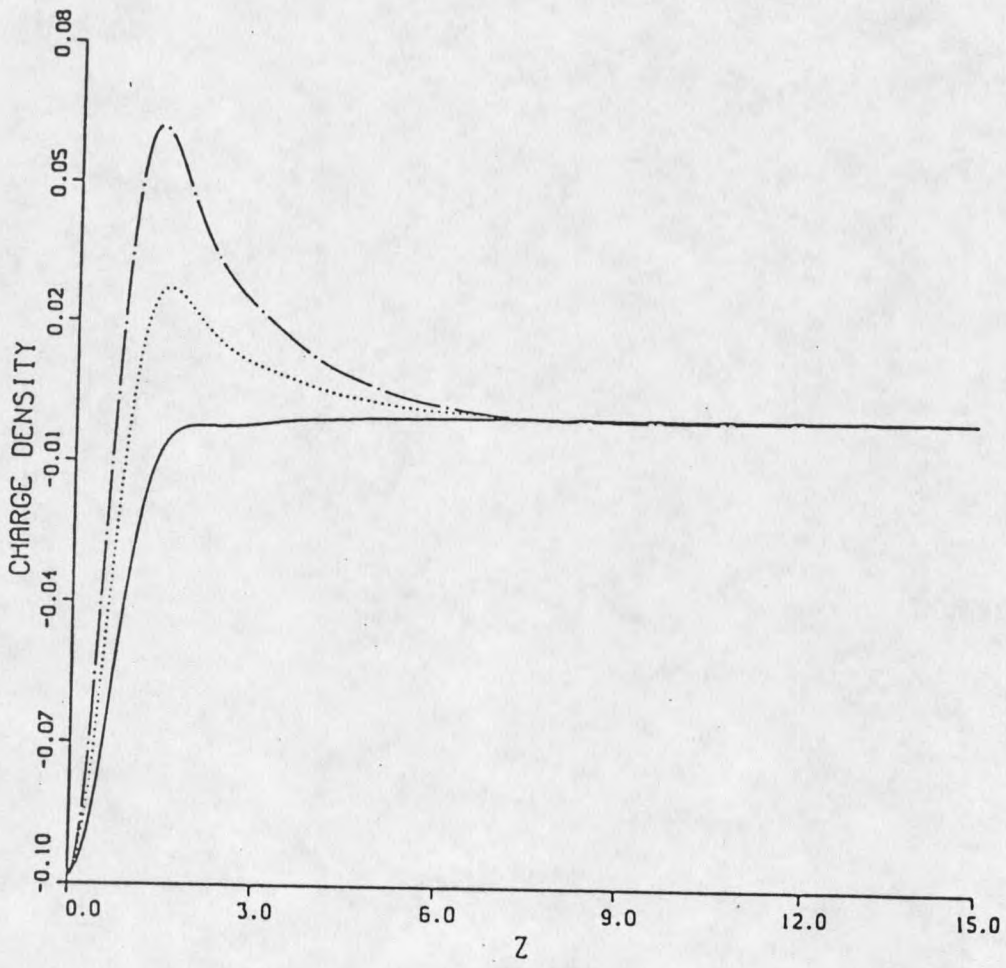

Fig. 2 Charge density profile for n = $1 \times 10^{18} cm^{-3}$. The solid line is for $Q_s = 0.08$, dotted line for $Q_s = 0.0$ and dotted-dashed line for $Q_s = -0.08$.

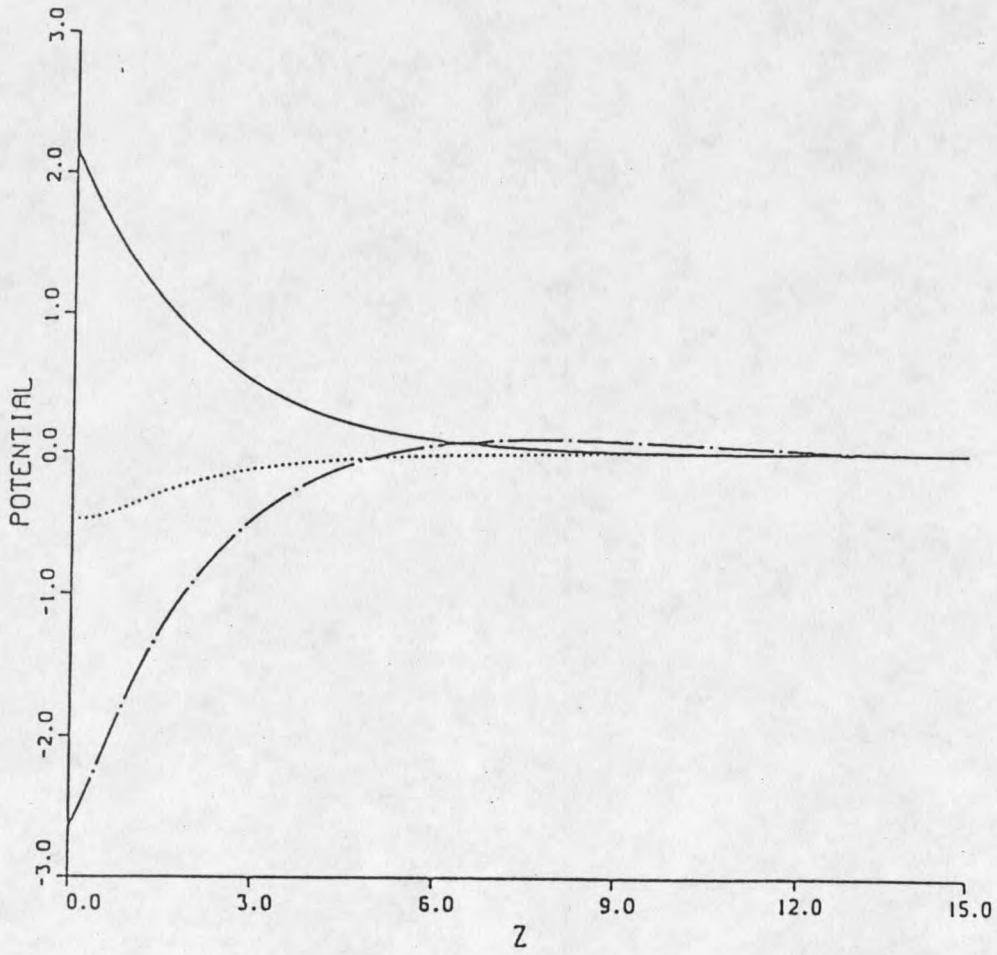

Fig. 3 Potential for $n = 3 \times 10^{17} cm^{-3}$. The solid line is for $Q_s = 0.08$, dotted line for $Q_s = 0.0$ and dotted-dashed line for $Q_s = -0.08$.

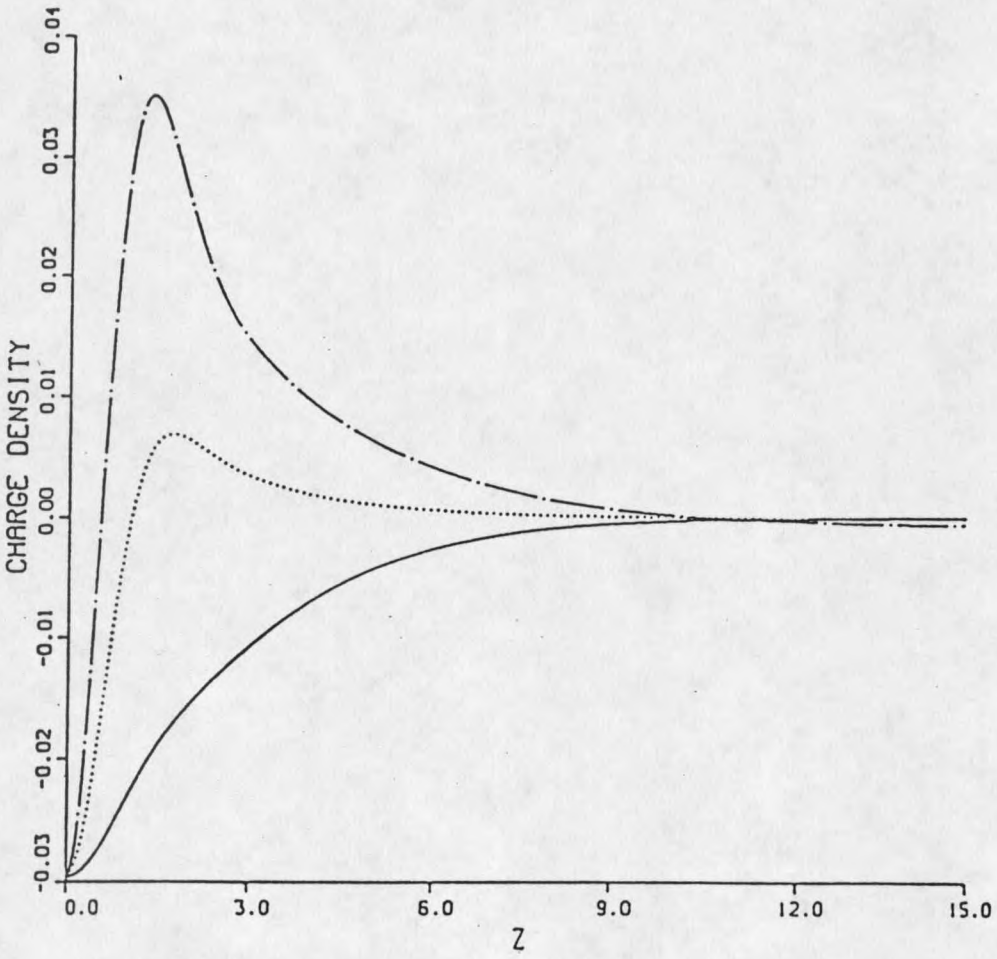

Fig. 4 Charge density profile for $n = 3 \times 10^{17} cm^{-3}$. The solid line is for $Q_s = 0.08$, dotted line for $Q_s = 0.0$ and dotted-dashed line for $Q_s = -0.08$.

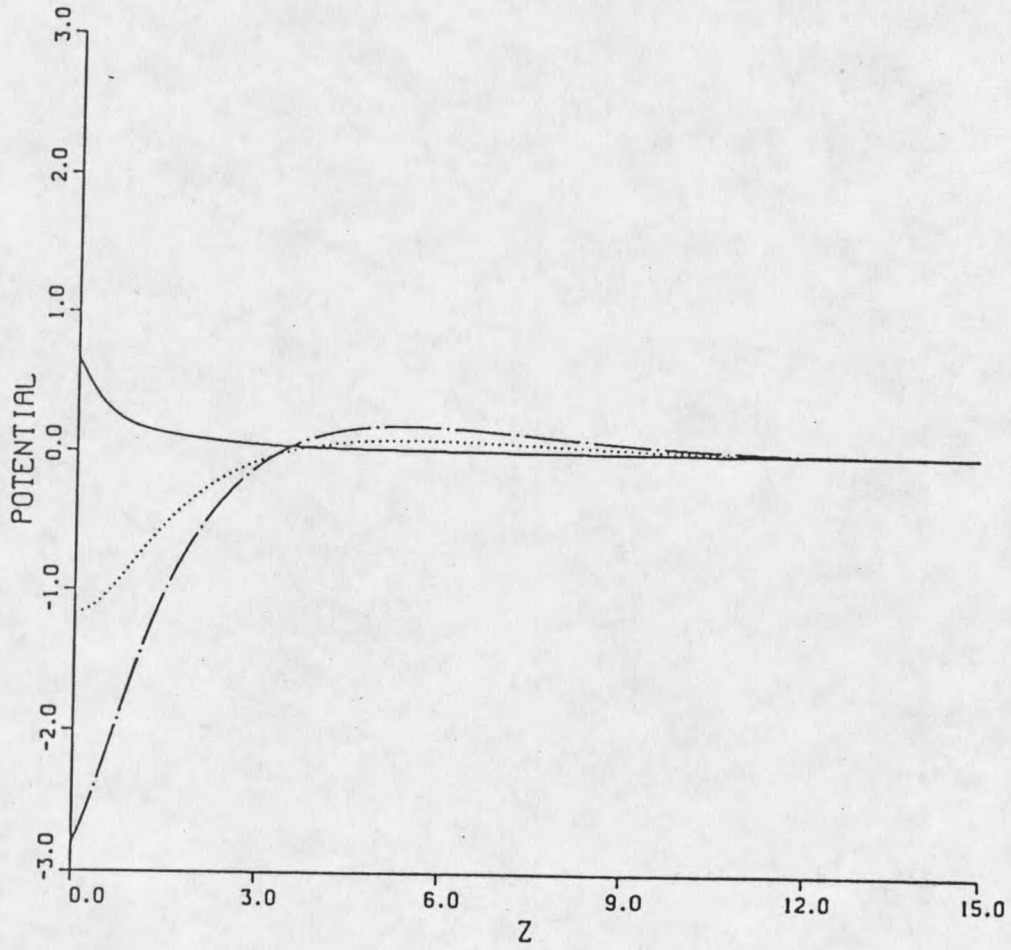

Fig. 5 Potential for n = 1 x 10^{18} cm^{-3}. The solid line is for Q_s = 0.08, dotted line for Q_s = 0.0 and dotted-dashed line for Q_s = -0.08.

Notice that rather strong accumulation layers have been explored in Fig. 3 and Fig. 5. For $n_0=3*10^{17}cm^{-3}$, and Q=-0.08 the maximum charge density in the accumulation layer rises to roughly two times the bulk value.

Comparing Fig. 3 with Fig. 5, it can be seen that as the carrier concentration n_0 increases, d decreases.

Spectra of $n_0=1.2*10^{18}cm^{-3}$ for different thicknesses of the depletion layer are shown in Fig. 6-Fig. 9. In each figure, there are three peaks. The middle one is the phonon peak, the others are the coupled plasmon and phonon peaks. Note that when $n_0=1.2*10^{18}cm^{-3}$, the plasmon energy is very close to the phonon energy thus leading to strong coupling. If the carrier concentration is very different from the value $n_0=1.2*10^{18}cm^{-3}$, just two peaks, i.e. the plasmon peak and the phonon peak, will be observed.[30] The surface mode frequency is given by

$$\omega_s^2 = 4\pi ne^2/[m^*(1+\varepsilon_\infty)]$$

with a free carrier concentration of $1.2*10^{18}cm^{-3}$, one evaluates the surface plasmon energy from above Eq. to be 44.9meV. The phonon energy is 36 meV. In Fig. 6, the thickness of the depletion layer is 50A, and three peaks are present at 29.4, 38.7and 47.1meV. The peak in the middle only appears as a shoulder. As the thickness of the depletion layer increases, the middle peak grows stronger, and the third peak becomes only a small shoulder, as shown in Fig. 7-Fig. 9. On the other hand, we find that when the thickness of the depletion layer increases from 50A to 100A, the lower energy peak shifts down about 2 meV and the third peak shifts down about 3 meV.

The qualitative features of the spectra in these figures can be understood in terms of depletion layer formation. The increase of the amplitude of the phonon loss

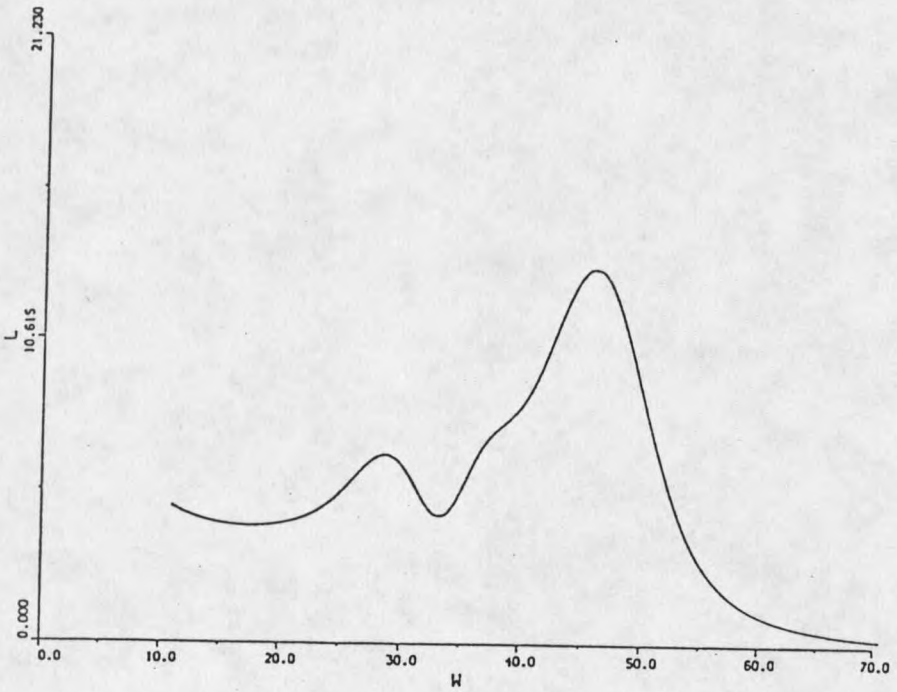

Fig. 6 Energy loss spectrum for $n_0 = 1.2 \times 10^{18} cm^{-3}$ and D (the thickness of the depletion layer) = 50 Å.

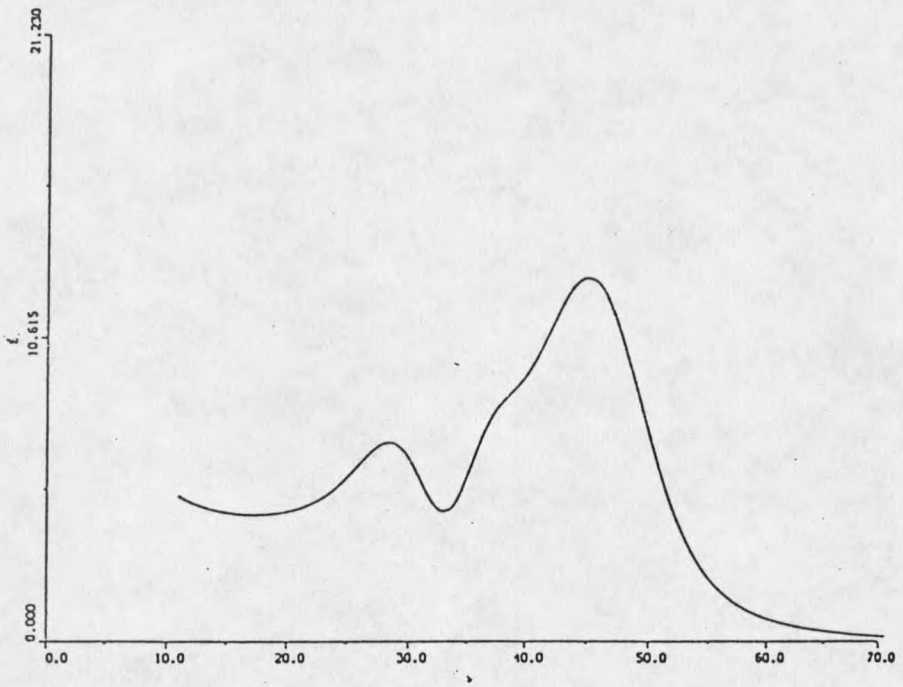

Fig. 7 Energy loss spectrum for $n_0 = 1.2 \times 10^{18} cm^{-3}$ and D (the thickness of the depletion layer) = 60 Å.

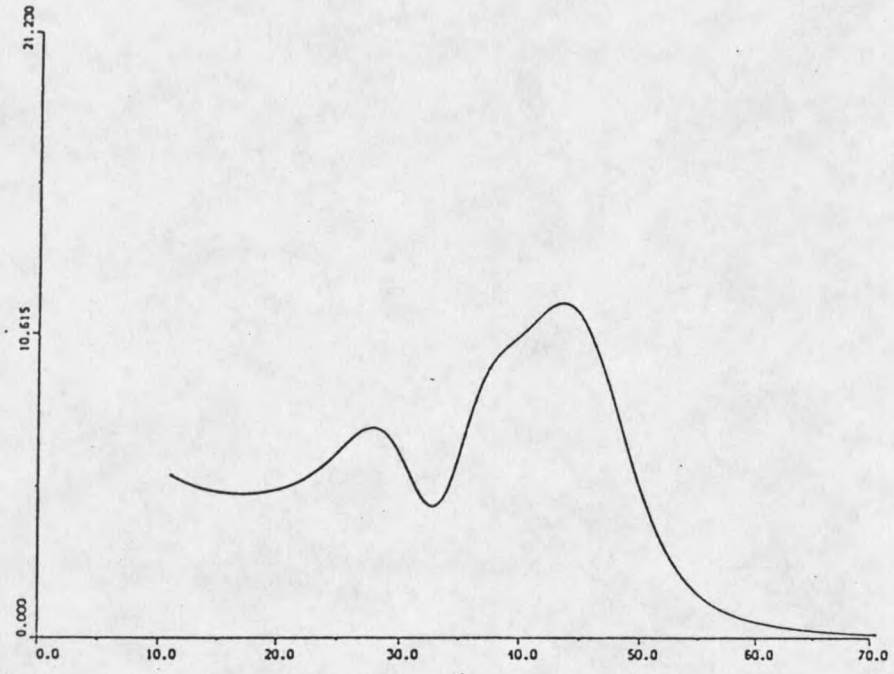

Fig. 8 Energy loss spectrum for $n_0 = 1.2 \times 10^{18} cm^{-3}$ and D (the thickness of the depletion layer) = 75 Å.

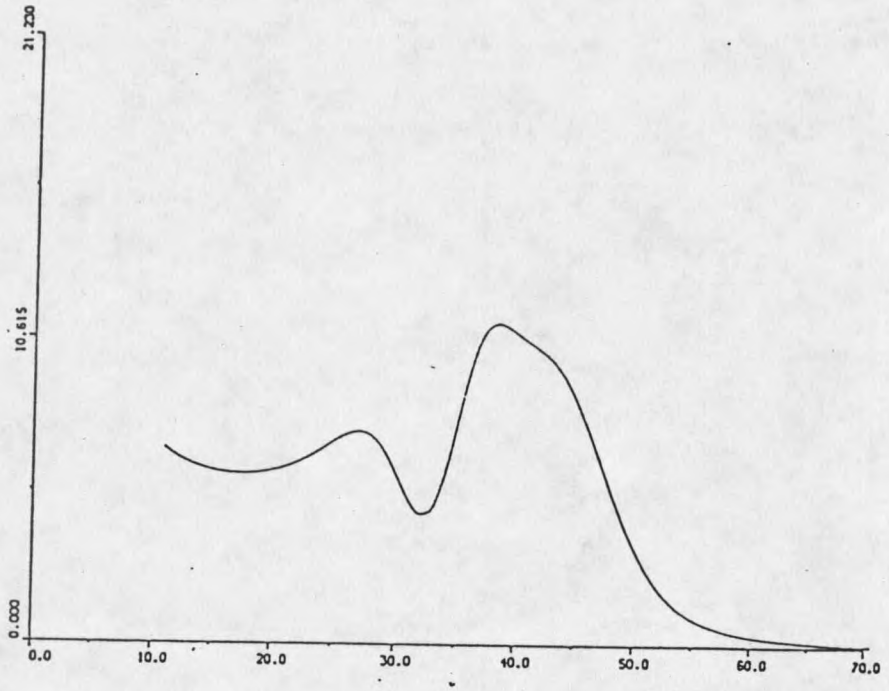

Fig. 9 Energy loss spectrum for $n_0 = 1.2 \times 10^{18} cm^{-3}$ and D (the thickness of the depletion layer) = 100 A.

peak is due to the increase of the depletion layer thickness. As the depletion layer thickness increases, a portion of the lattice vibrations is unscreened, making a stronger contribution to the loss spectrum. On the other hand background dielectric constant in the depletion layer is quite large (10.9 for GaAs), thus the plasmon eigen mode is strongly affected by ε_∞ and the thickness of the depletion region. Two extreme cases are considered. First, if the depletion layer is absent, $\omega_s=\omega_p/(\varepsilon_\infty+1)^{1/2}$ where ε_∞ is the high frequency limit of the dielectric constant. Second, for a infinitely thick depletion layer $\omega_s=\omega_p/(2\varepsilon_\infty)^{1/2}$. So, for a finite depletion layer thickness, the frequency (i.e. energy) of plasmon is between the two values. When the thickness of the depletion layer increases, the peak energy will shift down.

The results for other carrier concentrations are given in the Appendix.

Fig. 10-Fig. 12 show the position of the peak in the loss function as a function of k. The charge density profiles were shown in Fig. 2-Fig. 5. It is evident that as $k\rightarrow 0$, all frequencies lie near ω_s. When $n_0=1*10^{18}cm^{-3}$, the results of the TF(Thomas-Fermi) model and the DH(Debye-Huckel) model are very similar. But the slopes of the lines are smaller than Mills'. At $n_0=3*10^{17}cm^{-3}$, the results from the DH model is near Mills'. When $n_0=1*10^{17}cm^{-3}$, there is a large difference between the TF model and the DH model. For $Q_s=0$, the TF result is close to Mills' result, and for $Q_s=-0.08$, the DH result is close to Mills' result. For the three concentrations, the TF lines are all under the the DH and Mills lines. The DH lines sometimes lie below Mills' results, as for $n_0=1*10^{18}cm^{-3}$, sometimes near; as for $n_0=3*10^{17}cm^{-3}$ and sometimes above, as for $n_0=1*10^{17}cm^{-3}$. For both the TF and the DH model, the dispersion curves depend weakly on Q_s for fixed n_0. By contrast Mills' results are strongly affected by the Q_s value, especially for lower carrier concentrations.

Many other Figures have been obtained. They are presented in the Appendix.

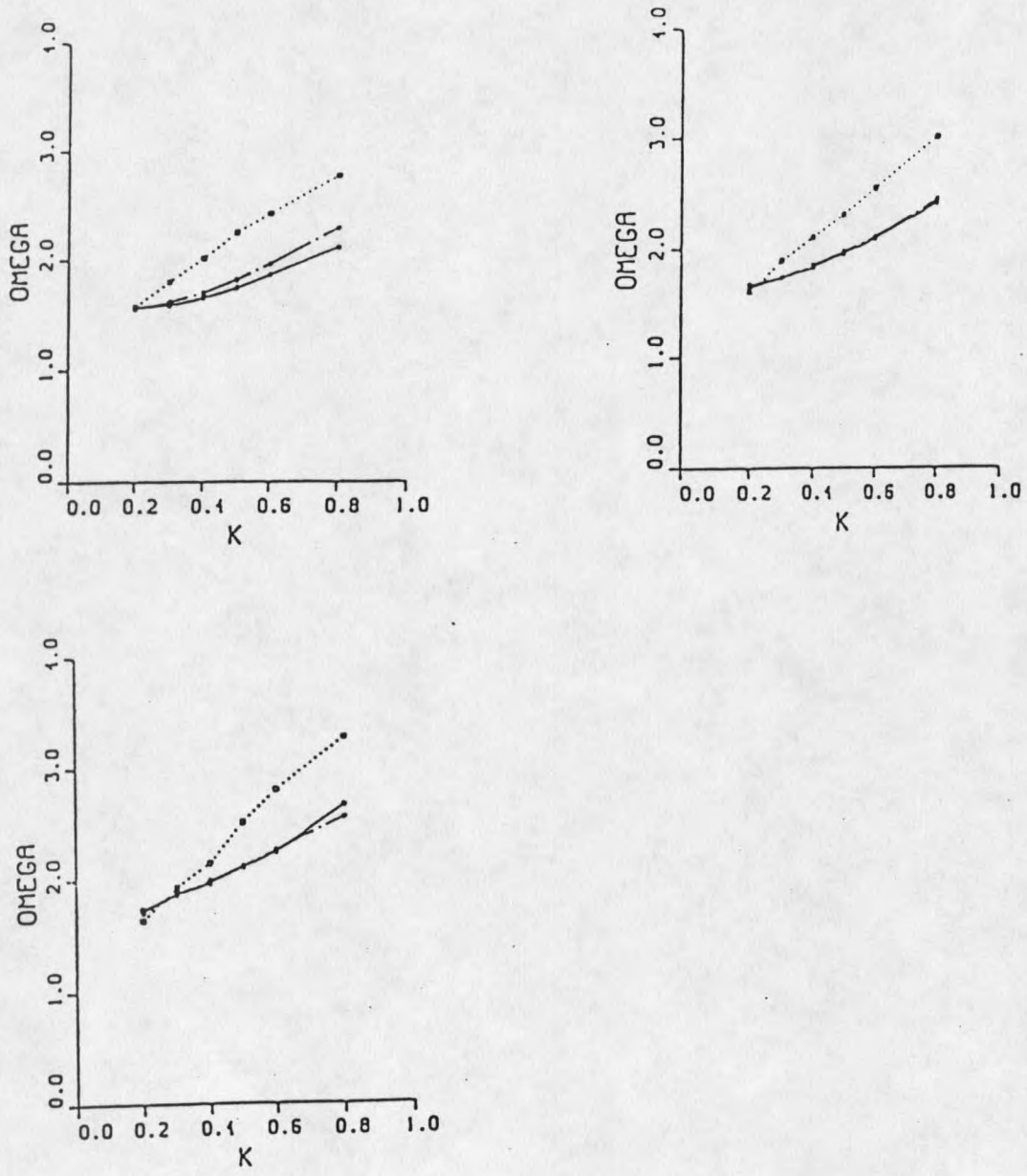

Fig. 10 Dispersion relations for a carrier concentration of $n_0 = 1 \times 10^{18} cm^{-3}$. Using the TF model and the DH model, we plot the position of the peak in the loss function as a function of K for different Q_s, namely $Q_s = 0.08$, $Q_s = 0.0$, and $Q_s = -0.08$. The results are compared with Mills' results. The solid line is for the TF results, dotted-dashed line for the DH results and dotted line for Mills' results.

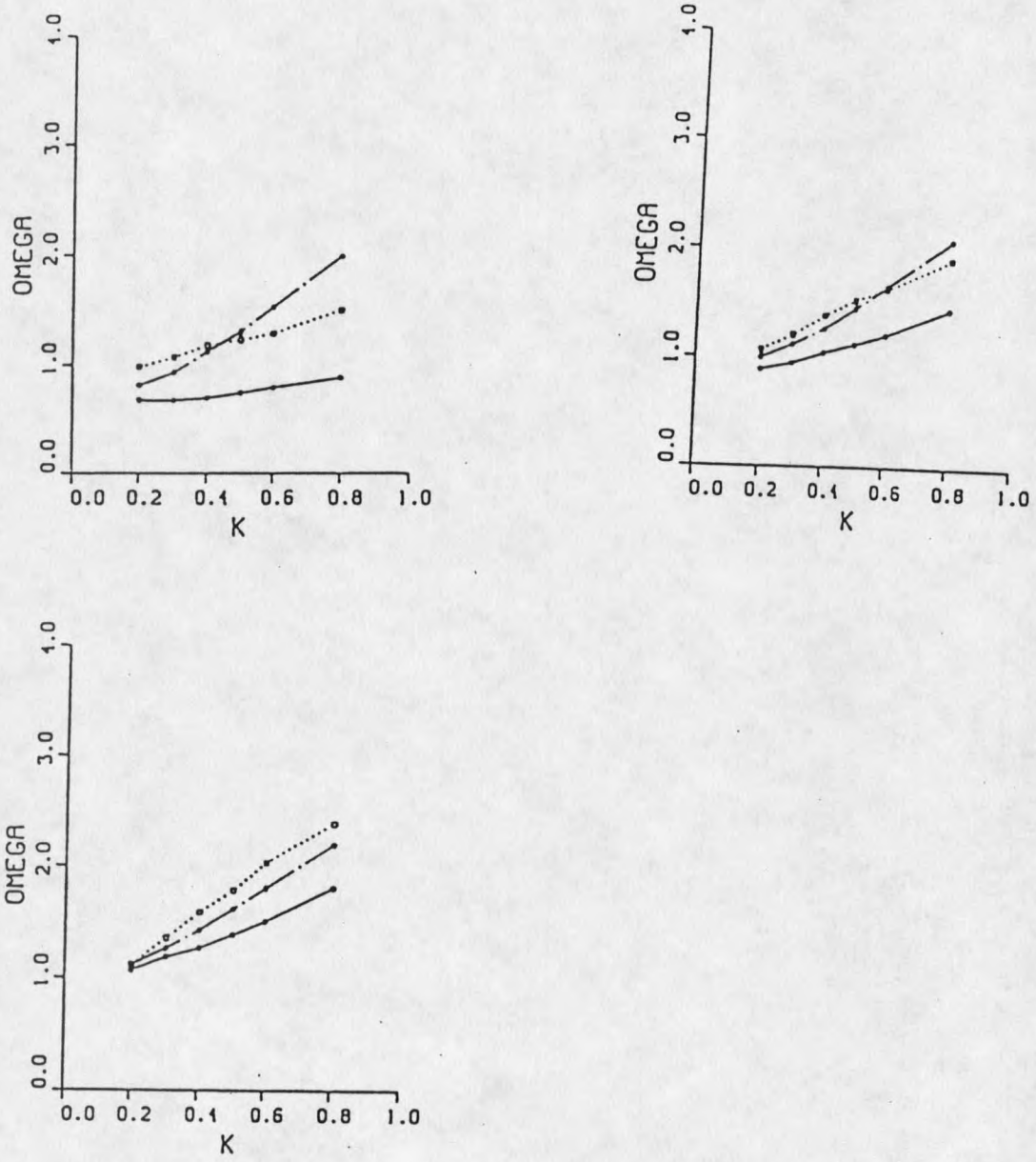

Fig. 11 Dispersion relations for a carrier concentration of $n_0 = 3 \times 10^{17} cm^{-3}$. Using the TF model and the DH model, we plot the position of the peak in the loss function as a function of K for different Q_s, namely $Q_s = 0.08$, $Q_s = 0.0$, and $Q_s = -0.08$. The results are compared with Mills' results. The solid line is for the TF results, dotted-dashed line for the DH results and dotted line for Mills' results.

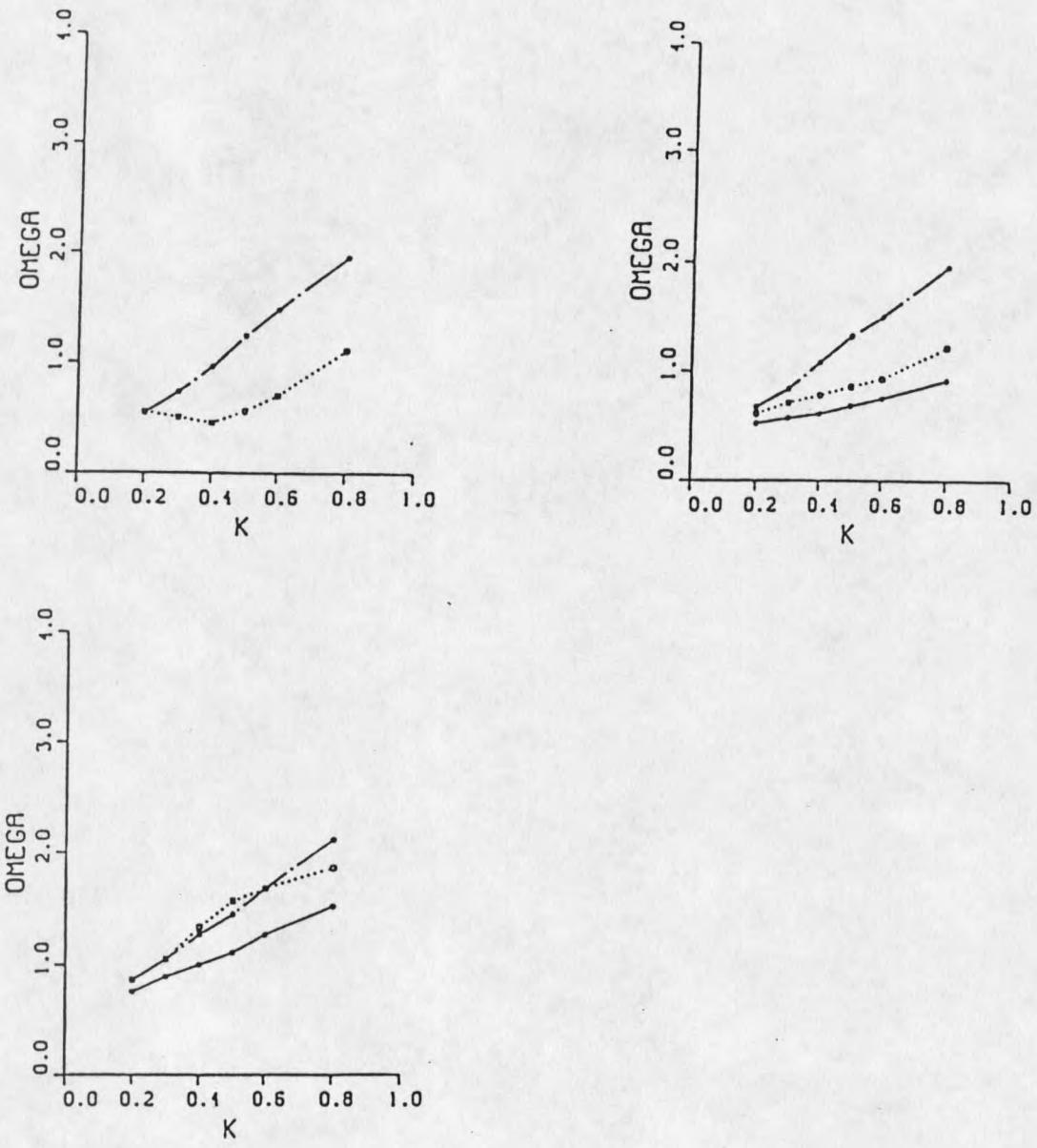

Fig. 12 Dispersion relations for a carrier concentration of $n_0 = 1 \times 10^{17} cm^{-3}$. Using the TF model and the DH model, we plot the position of the peak in the loss function as a function of K for different Q_s, namely $Q_s = 0.08$, $Q_s = 0.0$, and $Q_s = -0.08$. The results are compared with Mills' results. The solid line is for the TF results, dotted-dashed line for the DH results and dotted line for Mills' results.

Summary

We studied surface plasmons and phonons on n-type semiconductors, based on a simple picture of local dielectric response. By varying the model parameters we considered a wide range of free-carrier profiles associated with depletion and accumulation layers. The results for the frequency vs. wavevector curves of surface plasmons in our model were compared with those of Ehlers and Mills. The agreement was found to be reasonable although differences in detail occur because of the strong inhomogeneity of the charge density near the surface.

REFERENCES CITED

1. M. Liehr, P.A. Thiry, J.J. Pireaux, and R. Caudano, J. Vac. Sci. Technol. A2, 1079 (1984); Phys. Rev. B, 29 , 4824 (1984)

2. D.H. Ehlers and D.L. Mills Phys. Rev. B, 34, 3939(1986)

3. H. Ibach and D.L. Mills, Electron Energy Loss Spectroscopy (Academic, New York, 1982)

4. A.A. Lucas, J. P. Vigneron, Ph. Lambin, P.A. Thiry, M. Liehr, J.J. Pireaux, and R. Caudano, in Proceedings of the Sanibel Symposium, St. Augustine, 1985 [Int. J. Quantum Chem.]

5. Chapter 1 of "Solid State Physics" edited by Ashcroft and Mermin

6. Chapter 5 of "Quantum Theory of Many-Particle Systems" edited by Alexander L. Fetter and John Dirk Walecka

7. Chapter 9 of "Quantum Theory of Many-Particle Systems" edited by Alexander L. Fetter and John Dirk Walecka

8. Chapter 2 of "Dynamical Theory of Crystal Lattices" edited by Born and Huang

9. Ph. Lambin, J.P. Vigneron, and A.A. Lucas, Phys. Rev. B, 32, 8203(1985)

10. R.E. Camley and D.L. Mills Phys. Rev. B, 29, 1695(1984)

11. D.L. Mills Surf. Sci. 48 , 59(1975)

12. D.H. Ehlers and D.L. Mills, Phys. Rev. B, 36, 1051(1987)

13. G.A. Baraff and Joel A. Appelbaum Phys. Rev. B, 5, 475(1972)

14. N. Lang and W. Kohn, Phys. Rev. B, 1, 4555(1970)

15. Chapter 2 "Collective Effects in Solids and Liquids" edited by D.F. Brewer

16. Chapter 3 of "Optical Properties of Solids" edited by F. Wooten

17. Chapter 17 of "Solid State Physics" edited by Ashcroft and Mermin

18. Chapter 9 of "Optical Properties of Solids" edited by F. Wooten

19. Chapter 2 of "Dynamical Theory of Crystal Lattices" edited by Born and Huang

20. R.R. Gerhardts and K. kempa, Phys. Rev. B, 30, 5704(1984)

21. E. Evans and D.L. Mills, Phys. Rev. B, 5, 4126(1972)

22. A.A. Lucas and J.P. Vigneron, Solid State Commun. 49, 327(1984)

23. J.P. Vigneron, A.A. Lucas el. in Proceeding of the 17th International Conference on the Physics of Semiconductor, San Francisco, 209(1984)

24. A.A. Lucas and M. Sunjic, Prog. Surf. Sci. 2, 75(1972); Surf. Sci. 32, 439(1972)

25. H. Ibach and D.L. Mills, Electron Energy Loss Spectroscopy (Academic, New York, 1982)

26. S.L. Cunningham, A.A. Maradudin, and R.F. Wallis, Phys. Rev. B, 10 3342(1974)

27. E.M. Conwell, Phys. Rev. B, 11, 1510(1975)

28. Y.Chen, S. Nannarone, J. Schaefer, J.C. Hermanson and G.J. Lapeyre Phys. Rev. B, 39, 7653(1989)

29. Chapter 9 of "Quantum Theory of Many-Particle Systems" edited by Alexander L. Fetter and John Dirk Walecka

30. Y.Chen Ph.D. Thesis

31. Chapter 10 of "Introduction to Solid State Physics" edited by C. Kittle

32. Chapter 4 of "Surface Physics" edited by M. Prutton

33. Chapter 1 of "Theoretical Solid State Physics" edited by William Jones and Norman H. March

APPENDIX

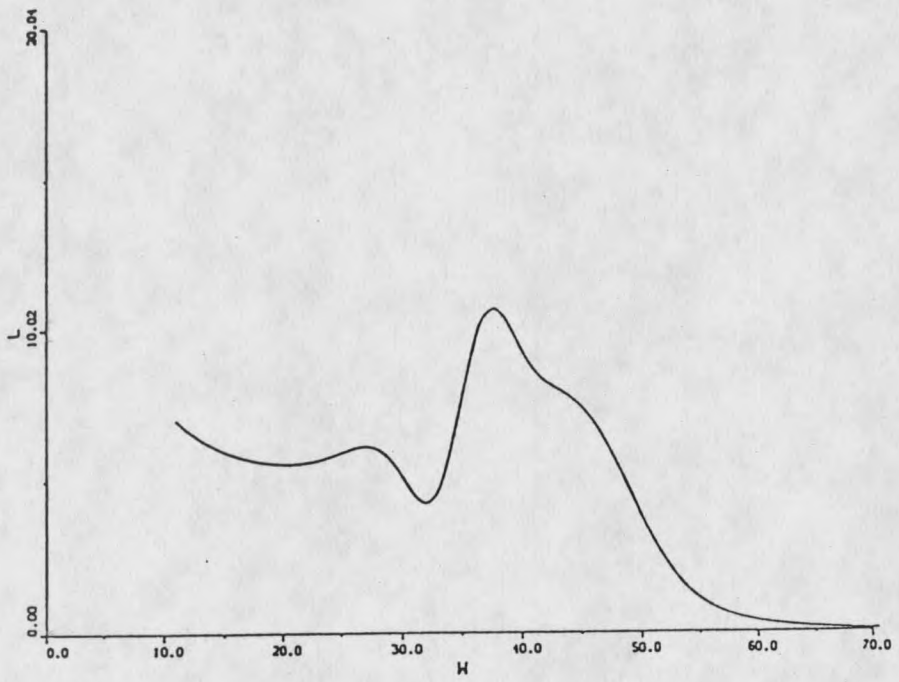

Fig. 13 Energy loss spectrum for n_0 = 1.35 x 10^{18} cm^{-3} and D (the thickness of the depletion layer) = 118 Å.

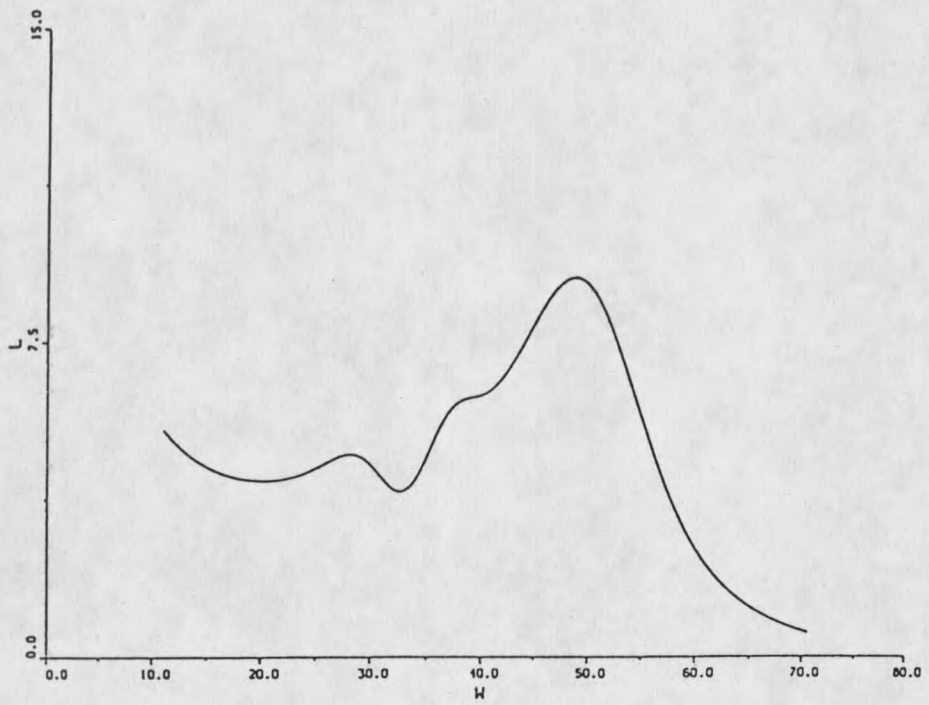

Fig. 14 Energy loss spectrum for n_0 = 1.5 x 10^{18} cm^{-3} and D (the thickness of the depletion layer) = 50 Å.

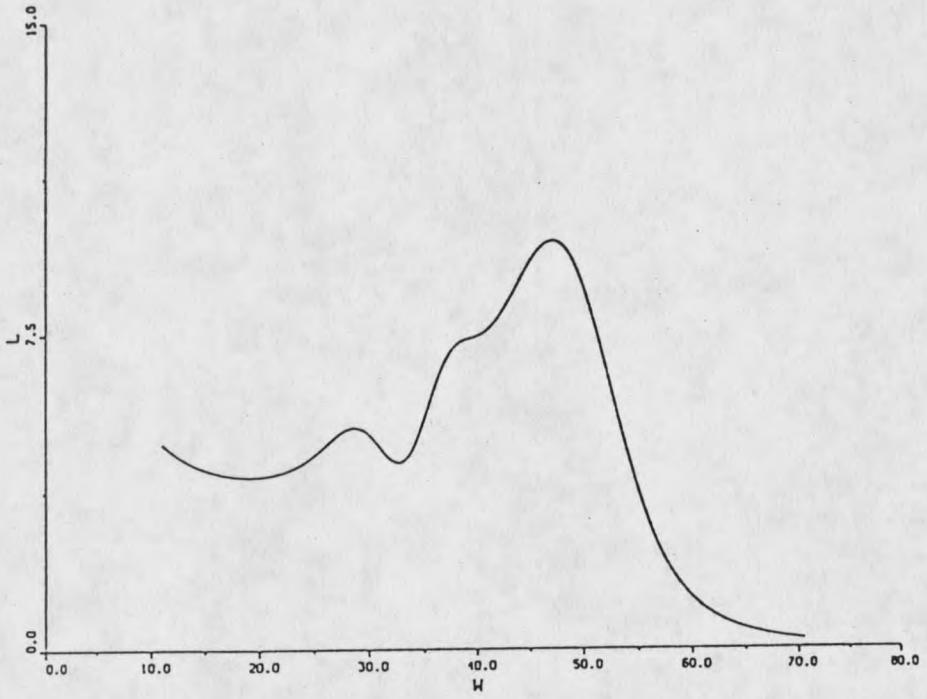

Fig. 15 Energy loss spectrum for n_0 = 1.5 x 10^{18} cm^{-3} and D (the thickness of the depletion layer) = 75 Å.